



Underwater Light Availability in Westcott Bay

Analysis of 2007-2008 Data from Three Stations

April 2009



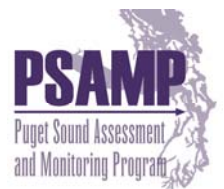
WASHINGTON STATE DEPARTMENT OF
Natural Resources
Peter Goldmark - Commissioner of Public Lands

Underwater Light Availability in Westcott Bay

Analysis of 2007-2008 Data from Three Stations

April 2009

by Pete Dowty and Lisa Ferrier
Nearshore Habitat Program
Aquatic Resources Division



WASHINGTON STATE DEPARTMENT OF
Natural Resources
Peter Goldmark - Commissioner of Public Lands

Acknowledgements

Jessie Lacy of the USGS was very helpful with suggestions on data cleanup and analysis, as well as the deployment of the instruments. Her specific suggestions on methods for data cleanup, the use of an error analysis and the use of nighttime PAR are very much appreciated.

The analysis reported here would not have been possible without the work of Anja Schanz, Jeff Gaeckle and Michael Friese (DNR) and Sandy Wyllie-Echeverria and Zach Hughes (Seagrass Lab at UW Friday Harbor Labs) who played a key role in maintaining the field instruments. Jeff Gaeckle also provided underwater photographs of the instruments.

Discussions with Jim Kaldy (EPA Newport OR), Blaine Kopp (USGS Augusta ME) and Ken Moore (Virginia Inst. of Marine Science) were very helpful in interpreting the results and putting them in a broader context of other studies of seagrass and light. Comments on an earlier draft from Megan Dethier (UW Friday Harbor Labs) were also very helpful.

Doug Bulthuis and Paula Margerum of the Padilla Bay National Estuarine Research Reserve were very generous with their time in discussing their deployment and use of YSI 6600 instruments.

We are grateful to Emily Carrington at UW Friday Harbor Labs, who makes surface PAR data, as well as other weather variables, available for download over the internet.

All contributors are DNR staff unless otherwise indicated.
Copies of this report may be obtained from the Nearshore Habitat Program –
Enter search term ‘nearshore habitat’ on DNR home page: <http://www.dnr.wa.gov>

Contents

EXECUTIVE SUMMARY	1
1 Introduction	3
2 Methods	5
2.1 Instruments	5
2.2 Deployment.....	5
2.3 Data Cleanup	7
2.4 Assessment of Daily PAR	8
2.4.1 Comparison of Daily PAR between Years and Months.....	9
2.4.2 Comparison of Daily PAR between Stations.....	10
2.5 Calculation of Attenuation	10
2.5.1 Comparison of Daily Attenuation between Years and Months.....	11
2.5.2 Comparison of Daily Attenuation between Stations	11
3 Results	12
3.1 Data Inventory.....	12
3.2 Daily PAR.....	12
3.2.1 Comparison of Daily PAR between Years and between Months.....	15
3.2.2 Comparison of Daily PAR between Stations.....	20
3.3 Attenuation.....	24
3.3.1 Comparison of Daily Attenuation between Years and between Months	24
3.3.2 Comparison of Daily Attenuation between Stations	28
4 Discussion	30
4.1 Does PAR Availability Match the Pattern of Eelgrass Loss?	31
4.2 Do Differences between Stations have Physiological Significance?	33
4.3 Lessons Learned – PAR Data from the YSI 6600 EDS Platform.....	35
5 Summary and Recommendations	37
6 References	39
APPENDICES	
Appendix A PAR Deployment Issues	43
A.1 Variation in Deployment Elevation	43
A.2 Unattached Sensor	52
A.3 Reversed PAR Connections	52

A.4	PAR Sensor Error Analysis.....	55
A.5	Correction for Reversed PAR Connections	57
A.6	Out-of-Water Observations.....	58
A.7	References	63
Appendix B PAR Data Cleanup		64
B.1	PAR Data Anomalies	64
B.2	Cleanup Algorithm	68
B.3	References	69



EXECUTIVE SUMMARY

The Washington State Department of Natural Resources (DNR) is steward of 2.6 million acres of state-owned aquatic land. DNR manages these aquatic lands for the benefit of current and future citizens of Washington State. As part of its stewardship responsibilities, DNR investigates the causes of observed losses in eelgrass in greater Puget Sound through the Eelgrass Stressor-Response Project.

Eelgrass (*Zostera marina*) is a flowering aquatic plant that supports nearshore food webs, provides habitat for many organisms, and is recognized as an indicator of ecosystem health. DNR has dedicated substantial effort to understanding the causes of the extensive *Z. marina* losses in Westcott Bay, San Juan Island. Westcott Bay was a herring spawning site, and it is one example of a regional pattern of *Z. marina* loss in shallow embayments in the San Juan Archipelago. Several groups are collaboratively investigating the loss, including the University of Washington Friday Harbor Labs, the USGS Pacific Science Center, Friends of the San Juans, and DNR. Identifying stressors related to observed *Z. marina* declines is an important first step toward formulating management responses to environmental degradation. Guidance regarding stressors of greatest concern is needed by multiple efforts to restore and protect Puget Sound, most notably the regional Puget Sound Partnership's Action Agenda.

The purpose of the work contained in this report was to quantitatively assess light limitation as a stressor that reduces the viability of habitat in Westcott Bay for *Z. marina*. Field observations of high water column turbidity at the head of Westcott Bay suggested the possibility that low light transmission through the water column may have played a role in the loss of *Z. marina* and continued lack of recolonization. The specific objectives were to assess two hypotheses related to light availability, which is measured as photosynthetically active radiation (PAR):

- H_1 : PAR is reduced in areas that have lost *Z. marina* relative to areas where *Z. marina* persists near the mouth of Westcott Bay at Mosquito Pass.
- H_2 : PAR levels in areas of *Z. marina* loss are less than the minimum PAR requirements reported in the literature for other sites.

To test these hypotheses, YSI instruments with sensors that continuously measure PAR were deployed at three stations in Westcott Bay in 2007 and 2008. Monitoring was conducted at the mouth of the bay at Mosquito Pass (station WP) where *Z. marina* beds are currently intact; an intermediate location at Bell Point that has experienced extensive *Z. marina* loss but supports a small residual bed (station BP); and the head of the bay where *Z. marina* has experienced a complete die-off (stations WBS and WBN).

Key findings include:

- PAR and attenuation observations indicate that PAR at the head of the bay is reduced relative to other points in the Westcott Bay area. In terms of mean daily PAR and season cumulative PAR, this reduction at the head of the bay is roughly 20%.
- The reduced average daily PAR at the head of the bay ($8.4 \text{ mol m}^{-2} \text{ day}^{-1}$) is still nearly threefold greater than the minimum requirements for *Z. marina* survival reported for *Z. marina* beds in Pacific Northwest estuaries ($3 \text{ mol m}^{-2} \text{ day}^{-1}$; Thom et al., 2008).
- Average daily PAR was indistinguishable between the mouth of the bay (WP) and Bell Point (BP). Average attenuation was also very similar between these two stations.

These findings strongly suggest that PAR is not an important controlling factor on *Z. marina* abundance in the Westcott Bay area. This conclusion is supported by the stark differences in *Z. marina* abundance and survival – *Z. marina* is abundant at the mouth of the bay and severely restricted at Bell Point, two sites with indistinguishable average levels of PAR.

In the course of this study, the Bell Point site emerged as a unique site given that it has experienced severe loss of *Z. marina* but still has a small residual bed. This *Z. marina* bed has high conservation value due to its rarity within Westcott Bay. It also provides a unique opportunity for future research to isolate stressors in this embayment.

This study was the Nearshore Habitat Program's first effort to deploy unattended PAR sensors and analyze the resultant datasets. Several methodological improvements were recommended for future projects, including conducting regular instrument intercomparisons, migrating to a more advanced analysis platform, and making the datasets easily available to other researchers.



1 Introduction

Eelgrass (*Zostera marina*) is a flowering aquatic plant that is common in marine nearshore subtidal and lower intertidal areas in greater Puget Sound. As a primary producer, it supports nearshore food webs and provides habitat for many organisms – including listed salmonids.

The Nearshore Habitat Program (NHP) of the Wash. Department of Natural Resources (DNR) has documented cases of eelgrass decline in greater Puget Sound through its annual monitoring project (Gaeckle et al. 2007). DNR initiated the Eelgrass Stressor-Response Project in 2005 to investigate causes of these declines (Dowty et al. 2007). Identifying stressors related to observed declines is an important first step toward formulating management responses to degradation. Guidance regarding stressors of greatest concern are needed by multiple efforts to restore and protect Puget Sound, most notably the regional Puget Sound Partnership's Action Agenda.

The loss of eelgrass at the head of Westcott Bay on San Juan Island has received considerable attention because it is a site of total loss and evidence suggests that it may be one example of a regional pattern of decline in shallow embayments of the San Juan Islands (Wyllie-Echeverria et al. 2003). Several groups are currently collaborating on investigations of the eelgrass loss in Westcott Bay including the University of Washington Friday Harbor Labs, the USGS Pacific Science Center, Friends of the San Juans, and DNR.

Observations of high turbidity at the head of Westcott Bay in 2006 suggested that low light transmission through the water column may have played a role in the loss of eelgrass and continued lack of recolonization (Kevin Britton-Simmons and Sandy Wyllie-Echeverria, pers. comm.). This report describes the deployment by DNR of YSI water quality monitoring instruments at three stations in Westcott Bay from 4/22/07 to 11/2/07 and again from 4/10/08 to 8/8/08. The report focuses only on the data collected by underwater PAR¹ sensors on the YSI instruments. The purpose of this work was to assess light limitation as a stressor that reduces the viability of habitat in Westcott Bay for eelgrass.

The objectives of this study were to assess two research hypotheses pertaining to PAR:

¹ Photosynthetically active radiation (PAR), the 0.4 – 0.7 μm portion of the solar spectrum.

H_1 : Reduction of PAR to levels insufficient to support eelgrass survival caused the loss of eelgrass in Westcott Bay.

H_2 : Current levels of PAR are insufficient to support eelgrass survival and prevent eelgrass recolonization in areas of loss.

Only H_2 can be directly assessed using current PAR conditions. In the absence of historical data, at best H_1 can be assessed indirectly, but cannot be formally tested. To address H_2 , it was broken down into two testable hypotheses:

H_{A1} : PAR is reduced in areas that have lost eelgrass relative to areas where eelgrass persists near the mouth of Westcott Bay at Mosquito Pass.

H_{01} : [null] There is no difference in PAR availability between areas that have lost eelgrass and areas that currently sustain eelgrass in Westcott Bay.

H_{A2} : PAR levels in areas of eelgrass loss are less than the minimum PAR requirements reported in the literature for other sites.

H_{02} : [null] PAR levels in areas of eelgrass loss are greater or equal to the minimum PAR requirements reported in the literature for other sites.

These hypotheses do not include specific PAR variables to be tested. Rather, they were used more generally to guide the analysis presented in this report.

2 Methods

2.1 Instruments

The PAR data were collected in Westcott Bay in the San Juan Islands with YSI 6600 EDS instruments with the dual PAR sensor kit offered by YSI. This instrument is unique in that it provides off-the-shelf capability to measure underwater PAR simultaneously at two depths, and the PAR sensors are automatically wiped to minimize biofouling during extended deployments. The PAR sensors used are the Li-Cor LI-192.

This configuration with PAR sensors only recently became available. It was developed through YSI collaboration with the Chesapeake Bay National Estuarine Research Reserve (Moore et al. 2004). It has since been deployed in other seagrass systems (Kopp and Neckles 2004).

The upper PAR sensor is denoted as the PAR1 sensor and the bottom sensor as PAR2. In addition to the PAR sensors, the instruments used in this study included YSI sensors measuring temperature, conductivity, pH, depth, dissolved oxygen, turbidity and chlorophyll, although data from these sensors are not considered here.



Figure 2-1. The YSI 6600 EDS with dual PAR kit (left) and a close-up of the lower PAR sensor and wiper with fouling accumulated over 3 weeks and 4 days in Westcott Bay.

2.2 Deployment

The YSI 6600 EDS instruments were deployed at three stations in Westcott Bay over a six-month period in 2007 and a four-month period in 2008. The three 2007

stations are denoted White Point (WP), Bell Point (BP) and Westcott Bay South (WBS), and their locations are shown in Figure 2-2. In 2008, YSI instruments were deployed at two stations that had been monitored in 2007 with YSI instruments (WP and BP), and a third station referred to as Westcott Bay North (WBN). The stations were selected to characterize a gradient in *Z. marina* condition as well as oceanographic and substrate properties (Grossman et al. 2007; Wyllie-Echeverria et al. 2003). WBS and WBN at the head of the bay have had total die-off of *Z. marina*. WP near the mouth at Mosquito Pass has the largest *Z. marina* bed of the three stations. BP has an intermediate position and has had significant *Z. marina* loss but currently supports a small, residual subtidal bed. The instruments were placed above sediment at -1.5 m MLLW as determined by the use of tables of predicted tide and measurements of water depth at the time of deployment. The instruments were placed vertically so that the lowest sensors on the YSI instrument were approximately 20 cm above the sediment surface. The lower PAR sensor was about 10 cm above these lowest sensors, and therefore about 30 cm above the sediment surface.

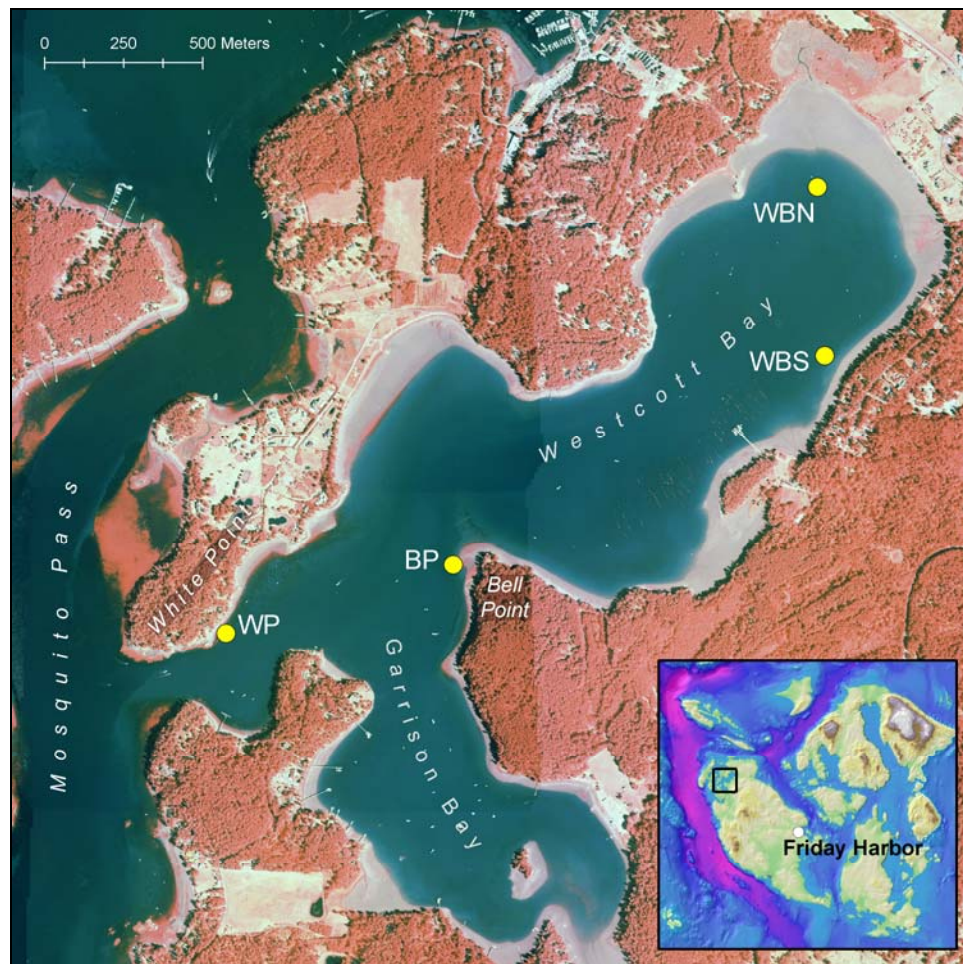


Figure 2-2. Map of Westcott Bay area with the locations of the three YSI deployments in 2007 (WP, BP and WBS) and 2008 (WP, BP and WBN).

The deployment apparatus was a modified version of the system used at the Padilla Bay National Estuarine Research Reserve. The instrument was lowered through a vertical 6-inch PVC tube to the deployment height. A slot was cut down the length of the tube to accommodate the PAR bracket (Figure 2-3). The PVC tube was attached to galvanized steel conduit that was driven into the sediment to provide support.

The positions of the PAR sensors on the PAR brackets were modified after delivery by YSI to allow the instrument to pass through the deployment tube. The vertical separation between the two sensors was 40.5 cm, except for one instrument that had 39.0 cm separation.

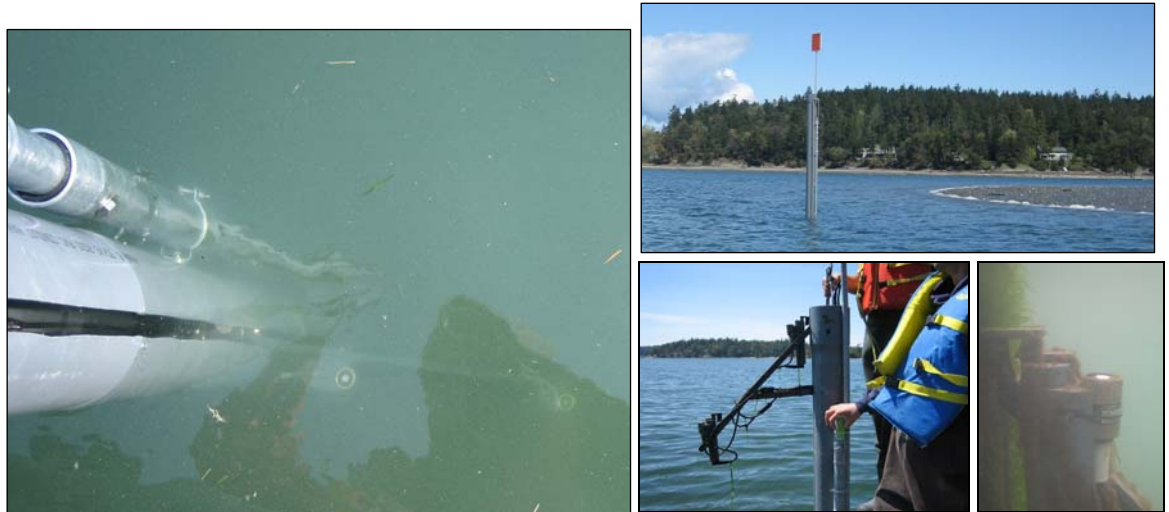


Figure 2-3. Deployment photos.

The instruments were retrieved approximately once a month for cleaning, data download and calibration. There was generally a 1-3 day data gap before the instruments were redeployed, although in one case this data gap reached 5 days.

2.3 Data Cleanup

Prior to analysis, the data were passed through several processing steps to address specific deployment issues and unexplained data anomalies. These steps are described in detail in appendices and only summarized here.

These initial processing steps led to an adjustment of some data values and elimination of others. Data were adjusted for deployments where PAR1 and PAR2 cables had been reversed (Appendix A.3, p.54). Data were eliminated in one deployment with an unattached and downward facing PAR sensor (Appendix A.2, p.54), and other deployments where PAR wipers were malfunctioning and a clear effect on the data was observed (all such eliminated data indicated in Figure 3-1).

Additional data processing addressed patterns in the data that could not be definitively explained but were considered anomalies. Three unexplained patterns in the data were identified for cleanup:

- Negative attenuation coefficients with values less than could readily be explained by instrument error;
- Significant increments in PAR of opposite sign in the PAR1 and PAR2 sensors from one observation to the next;
- Apparent signal loss where there was an abrupt decline in observations of mid-day PAR to unrealistically low values with little or no variation before an abrupt return to expected values. During subsequent servicing of the instruments by YSI to address this issue, intermittent connections within the PAR electronics were isolated. These connections likely caused the signal loss observed.

Examples of these unexplained patterns are shown in Figure B-1 (p.68). The cause of these patterns remains unresolved but likely involves some combination of the following factors:

- Random errors in the Li-Cor sensor due to finite precision. Precision is not characterized in the Li-Cor literature and was not addressed on the phone by Li-Cor technical staff. Given the simplicity of the sensor itself, and segments of uniform data in low-light conditions (Figure B-2, p.69), it seems unlikely that this plays a significant role.
- Problems in the YSI signal processing and logging system. Irregularities in the low-light data (Figure B-2, p.69) and consultations with other researchers suggest that this is a possibility with reasonable likelihood.
- Sensor obstruction. This could be caused by intermittent covering of the sensor by plants and algae that are attached to the instrument or deployment apparatus. It could also be caused by the temporary settling of floating detritus on the sensor. Given field observations of attached plants and algae on these instruments, and of floating debris in Westcott Bay, some level of sensor obstruction is almost certain.

Regardless of the sources of these patterns in the data, they were considered anomalies and they were removed from the data through the use of a cleanup algorithm and manual inspection for the signal loss pattern. Bad data points were removed and were subsequently replaced with linearly interpolated values if (a) no more than 20% of the daylight data points for the day were bad and (b) there were no more than two consecutive bad data points. Bad data points that did not meet these two criteria were replaced with a bad data flag (-9999). Additional details are described in Appendix section B.2 (p.71).

During the course of the analysis, it became clear that the deployment elevation varied across stations and even across individual deployments. It is impossible to fully correct the data for this issue, but the effect on the data was assessed in Appendix A.1 (p.44).

2.4 Assessment of Daily PAR

Daily PAR is the integral of PAR quanta received on a horizontal surface throughout the day. It was estimated for stations on days with good PAR data throughout the daylight hours. Daylight hours were taken to be those between daily sunrise and sunset at Friday Harbor that was obtained in Pacific Standard Time from the US Naval Observatory (http://aa.usno.navy.mil/data/docs/RS_OneYear.php).

Daily PAR, I_d , was estimated using only daylight PAR measurements as

$$I_d = \left(\sum I_i \right) \left(60 \frac{\text{sec}}{\text{min}} \right) (F)$$

where the sum is only over daylight hours of individual PAR measurements I_i . The sampling interval, F , in 2007 was 30 minutes for measurements prior to June 16, 2007 and 15 minutes from June 16 forward. In 2008, the sampling interval was 15 minutes throughout.

2.4.1 Comparison of Daily PAR between Years and Months

To compare available PAR in 2007 to that in 2008, average daily PAR values were calculated for each day for each station and each sensor (upper and lower). The overall difference between years was tested for significance with a two-way ANOVA with year and station as factors. PAR1 and PAR2 results were tested separately. For this analysis, data from stations WBS (2007) and WBN (2008) were combined to represent conditions at the head of the bay. Data used in the ANOVAs were restricted to the sampling period common to both years. These ANOVAs with unequal replication were run using Statistica (StatSoft Inc.).

Monthly average daily PAR values were also calculated and plotted for each station and each sensor. The data used to calculate these averages were still restricted to the sampling period common to both years. Differences in months were tested with an unequal replication multiple ANOVA with month, year and station as factors (Statistica, StatSoft Inc.). Again, data from stations WBS (2007) and WBN (2008) were combined to represent conditions at the head of the bay.

An independent assessment of PAR differences between 2007 and 2008 was conducted using simulated submarine PAR data based on surface PAR data and tidal height observations collected at Friday Harbor. Conditions at Friday Harbor likely diverge somewhat from those at Westcott Bay, being 12 kilometers distant and on the opposite side of San Juan Island. However, the Friday Harbor data records benefit from virtually no missing data, and it is reasonable to assume that any significant differences between years at Friday Harbor would also affect Westcott Bay.

The Friday Harbor PAR data were obtained from the Carrington Lab at Friday Harbor Laboratories at a frequency of 15 minutes (http://depts.washington.edu/fhl/fhl_wx.html). The tidal height observations were obtained from NOAA at a frequency of one hour (<http://tidesandcurrents.noaa.gov>, station 9449880). The tide data were linearly interpolated to 15 minute frequency

to match the PAR data. At each 15 minute sample time between 4/1 and 8/31 for each year, submarine PAR was simulated at a depth of -1.5m MLLW by calculating the height of the overlying water column (given the tide). The PAR at depth was then calculated as the residual PAR quantum flux when the incident surface PAR (from FHL) was attenuated through the water column according to Beer's Law with a constant attenuation coefficient of 0.5 m⁻¹. This attenuation is within the range of mean attenuation observed in Westcott Bay (below). The two years of simulated submarine PAR were tested for significant difference using a one-way ANOVA with year as factor, and a two-way ANOVA with year and month as factors (equal replication ANOVAs conducted with Microsoft Excel).

2.4.2 Comparison of Daily PAR between Stations

To compare available PAR across stations, the mean daily PAR over 2007-2008 was calculated for each station by pooling data from both 2007 and 2008. Only days with contemporaneous data across the stations were considered. This allowed for analysis with a repeated measures ANOVA (Microsoft Excel) to test for significant differences between stations. The Tukey test was used for multicomparison follow-up tests (Zar 1999, p.210). For this analysis, data from stations WBS (2007) and WBN (2008) were combined to represent conditions at the head of the bay.

2.5 Calculation of Attenuation

The simultaneous PAR1 and PAR2 data were used to calculate attenuation for those observations within three hours of solar noon (i.e. a six-hour window). The attenuation coefficient was calculated for each observation considered as well as on a daily basis. Data collected at low sun angles was not considered due to the longer light path in the water and altered relative path lengths for light reaching the PAR1 and PAR2 sensors. This tends to decrease the apparent attenuation (Carruthers et al. 2001).

This sun altitude effect is minimal in turbid water, but Kirk (1977, 1984) recommends restricting measurements to within 2 hours of solar noon in clear water conditions. Others generally recommend using data within 3 hours of solar noon, and that was the method used here (Blaine Kopp, USGS Patuxent Wildlife Research Center, pers. comm.).

The civil time (PDT) of solar noon was estimated on a daily basis as the midpoint between Friday Harbor sunrise and sunset obtained in PST from the US Naval Observatory (http://aa.usno.navy.mil/data/docs/RS_OneYear.php).

Attenuation was calculated from Beer's Law, $I_2 = I_1 e^{-kd}$, as

$$k = -\frac{\ln\left(\frac{I_2}{I_1}\right)}{d} \quad (\text{Eqn 2-1})$$

Where

k is the attenuation coefficient [m⁻¹]

I_2 is the PAR irradiance measured by the PAR2 (lower) sensor [$\mu\text{mol m}^{-2} \text{s}^{-1}$],
 I_1 is the PAR irradiance measured by the PAR1 (upper) sensor [$\mu\text{mol m}^{-2} \text{s}^{-1}$],
 d is the vertical distance separating the two sensors [m].

Individual pairs of PAR measurements within the ± 3 hour time window around solar noon were used in Equation 2-1 to calculate attenuation for each sampling time. These discrete attenuation values were only used as a check on data quality in the data cleanup process.

2.5.1 *Comparison of Daily Attenuation between Years and Months*

Daily attenuation was calculated with equation 2-1 using the sum of PAR1 and the sum of PAR2 within each day's ± 3 hour time window around solar noon (following Blaine Kopp, pers. comm.). These results were tested for significant differences between years with an unequal replication two-way ANOVA with year and station as factors (Statistica, StatSoft Inc.). The data for this analysis were restricted to the common sampling period between years (4/21 – 8/8).

Monthly and seasonal average attenuation were calculated as simple arithmetic means of the daily attenuation values. Monthly differences were examined with an unequal replication multiple ANOVA with month, year and station as factors (Statistica, StatSoft Inc.). Again, the data were restricted to the common sampling period (4/21 – 8/8).

2.5.2 *Comparison of Daily Attenuation between Stations*

Station differences were examined by combining data from 2007 and 2008 and conducting a repeated measures ANOVA with day and station as factors (Microsoft Excel). Only days with contemporaneous data across the stations were considered. The Tukey test was used for multicomparison follow-up tests (Zar 1999, p.210). For this analysis, data from stations WBS (2007) and WBN (2008) were combined to represent conditions at the head of the bay.

All confidence intervals presented are based on a t distribution.



3 Results

3.1 Data Inventory

Figure 3-1 shows the scope of the data collection at the three stations. Data collection in 2007 started on 4/21/07 and ended on 11/2/07. In 2008, data was collected from 4/10/08 to 8/8/08. The common period between the two years was then 4/21 to 8/8. Regular gaps in the data reflect maintenance time for instrument retrieval, cleaning, data download and calibration. Five different instruments were used over the entire data collection. The data cleanup reduced the amount of usable data, particularly for analyses that require contemporaneous data across all three stations.

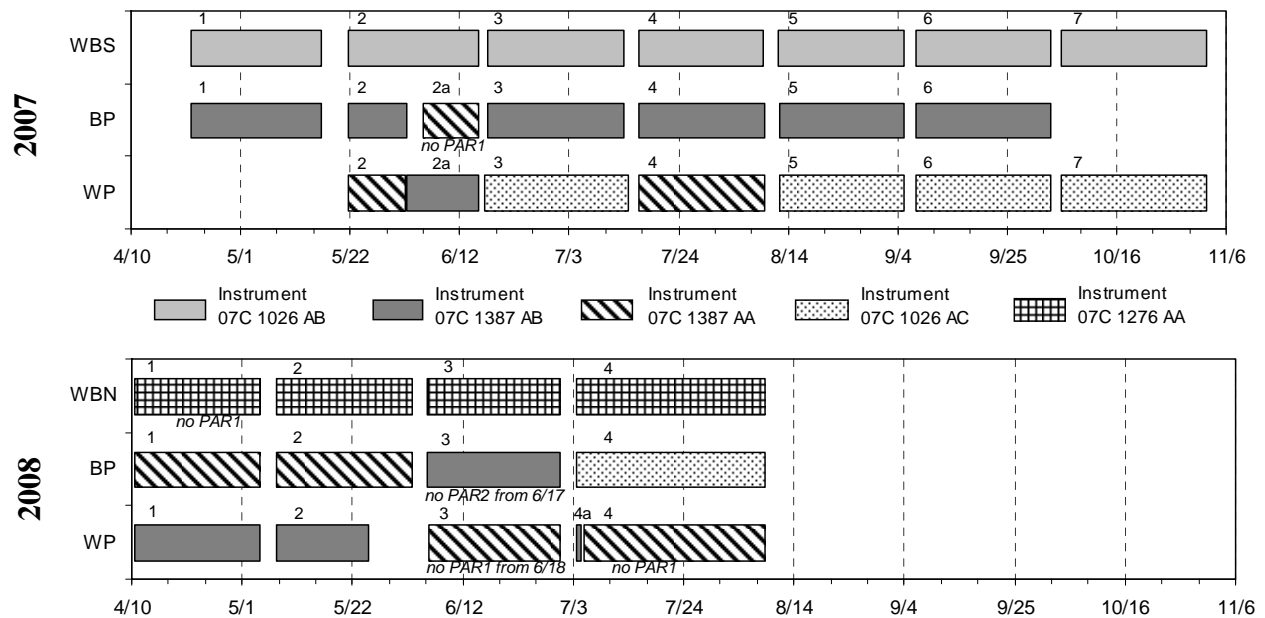


Figure 3-1. Data coverage in 2007 (top) and 2008 (bottom) using five different YSI 6600 EDS instruments. Each discrete deployment period was assigned a number that appears above each bar. Notes under the bars indicate specific deployments where data was removed due to instrument problems.

3.2 Daily PAR

The daily PAR results are shown in Figure 3-2 and Figure 3-3. The data points with contemporaneous data across the three stations are distinguished from data points without corresponding data at the other stations. It is clear that the

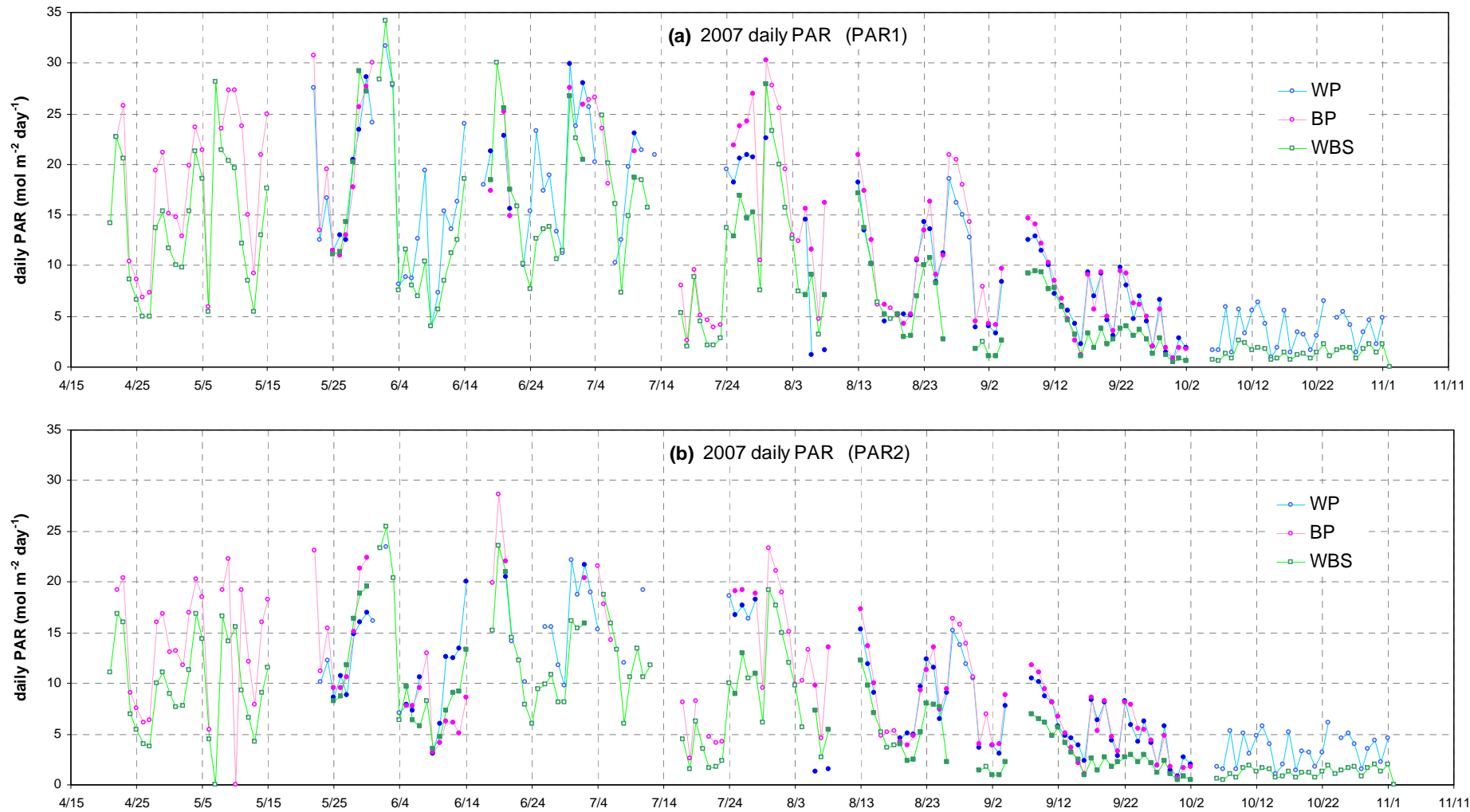


Figure 3-2. 2007 daily PAR as estimated by data from the (a) PAR1 and (b) PAR2 sensors at WP, BP and WBS stations. Only days with complete data between sunrise and sunset are shown and the daily estimates are based on these daylight data only. Days with contemporaneous daily PAR estimates at all three stations are shown as solid circles. Hollow circles indicate that data are missing for one or both of the other stations for that day (limiting direct comparisons across stations).

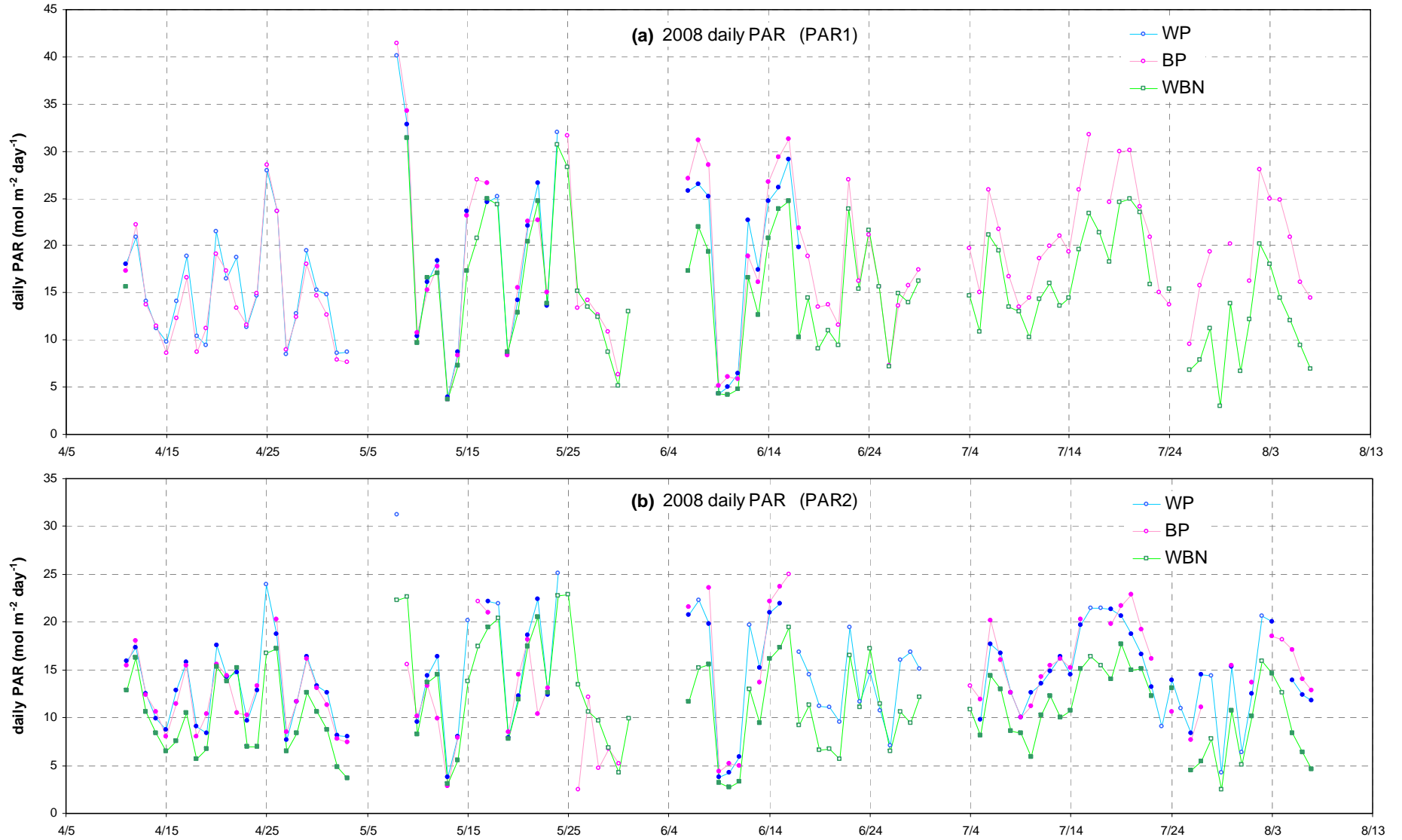


Figure 3-3. 2008 daily PAR in the same format as Figure 3-2. Note the extended y-axis in (a).

contemporaneous data are not uniformly distributed through the data record (see also Figure 3-5). There is a clear reduction in daily PAR from mid-August through the end of the 2007 data series for both PAR1 and PAR2 sensors. In 2008 the data record ends before this reduction would have been observed. The stations at the head of the bay (WBS and WBN) clearly tend to have lower daily PAR values in both years.

3.2.1 Comparison of Daily PAR between Years and between Months

Figure 3-4 compares the average daily PAR over the common sampling period (4/21 – 8/8) between years for each station. The daily PAR data available for these averages were not uniformly distributed through the common sampling period. For example, the 2007 data from WP do not include any values from April or early May (Figure 3-5).

The PAR2 averages are clearly reduced relative to the PAR1 averages. Differences in average daily PAR between years appear minor relative to the 95% confidence intervals. This is confirmed by the two-way ANOVA with year and station as factors which shows no significant effect ($\alpha=0.05$) associated with year (Table 3-1). Differences between stations were significant, but a later test (Table 3-4, p.20) provides a more robust assessment of differences between stations. This test, however, is the best single test for differences between years in average daily PAR.

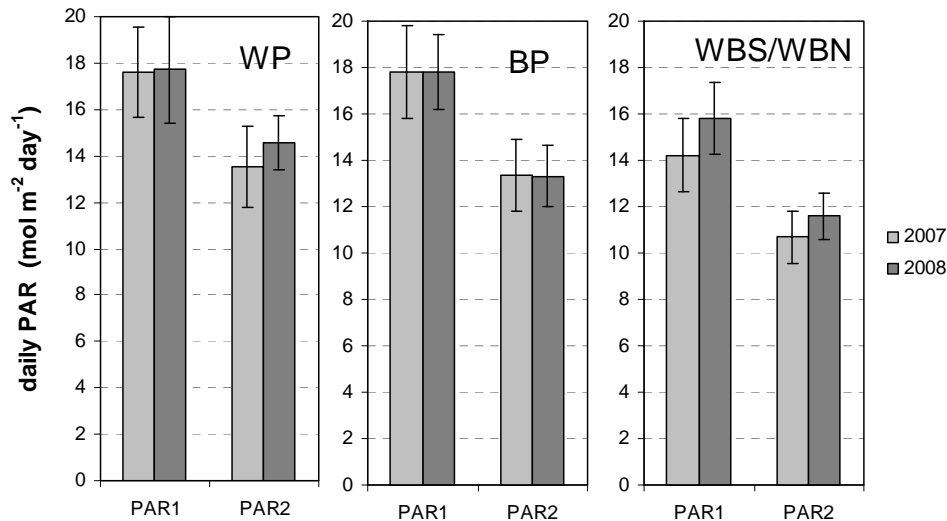


Figure 3-4. Comparison of average daily PAR across years. Daily PAR was averaged only over the period that was sampled in both years (April 21 – August 8). The distribution of data with each year varies across the stations, so differences between stations should be interpreted cautiously (see Figure 3-5) Error bars are 95% confidence intervals on the means. Sample sizes range from 41 to 94 days for the averages.

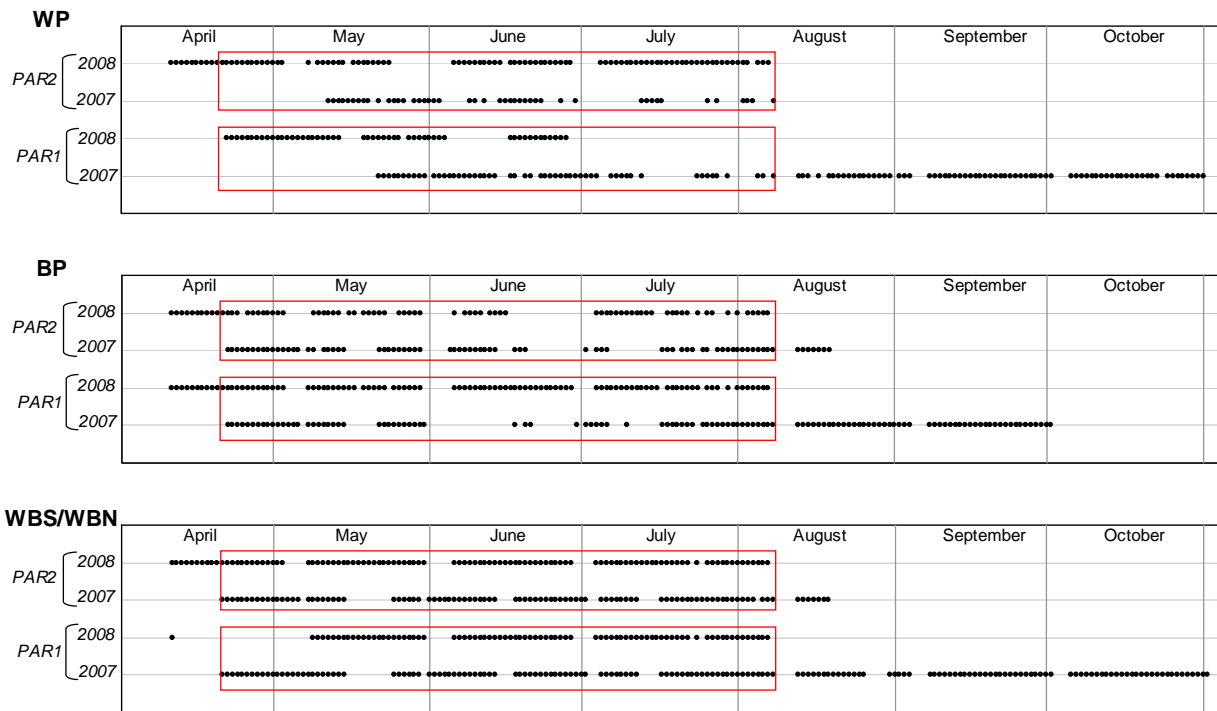


Figure 3-5. The distribution of daily PAR data available for analysis. The red boxes delineate the dates of sampling that were common to 2007 and 2008, April 1 to August 8.

	<i>Source of Variation</i>	<i>SS</i>	<i>df</i>	<i>MS</i>	<i>F</i>	<i>P-value</i>
PAR1 ANOVA	Year	70.6	1	70.6	1.255	0.263311
	Station	1110.3	2	555.1	9.873	0.000065
	Interaction	3.4	2	1.7	0.030	0.970108
	Within	23279.2	414	56.2		
PAR2 ANOVA	Year	55.11	1	55.11	1.796	0.180897
	Station	771.36	2	385.68	12.569	0.000005
	Interaction	9.67	2	4.84	0.158	0.854222
	Within	13379.2	436	30.69		

Table 3-1. ANOVA tables testing for significant differences ($\alpha=0.05$) in average daily PAR between years and between stations. The data are restricted to days with contemporaneous data across stations in the 4/21 – 8/8 period. The data are summarized in Figure 3-4. PAR1 (top) and PAR2 (bottom) data were analyzed separately.

There were also no obvious differences between years in monthly average daily PAR (Figure 3-6). These results should be interpreted with caution given some relatively low sample sizes and the particularly poor representation of the months of August (8/1 – 8/8) and April (4/21 – 4/30). Month did not have a significant effect in a multiple ANOVA (not shown) with month, year and station as factors for either the PAR1 or PAR2 analysis. To ensure reasonable coverage across all three stations, this analysis was restricted to May-June for PAR1 and May-June-July for PAR2. The station factor was significant for both PAR1 and PAR2, and the month-year-station interactions were significant in the PAR2 analysis.

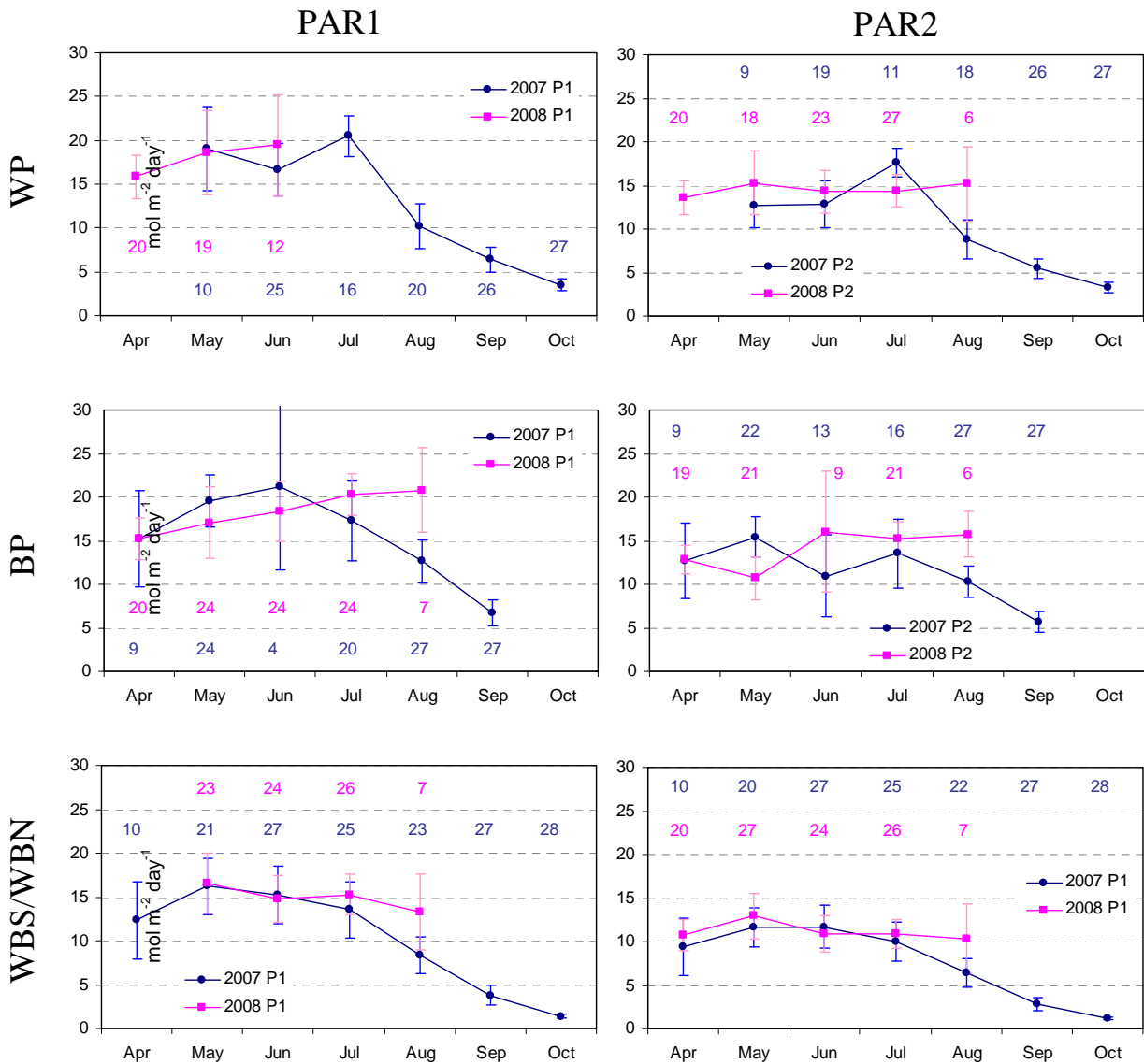


Figure 3-6. Comparison between 2007 and 2008 of monthly averages of daily PAR. Error bars are 95% confidence intervals. All available data were used to compute these averages. These values therefore do not represent the input data to the ANOVA in Table 3-1, which was a subset of the data shown here. Blue numbers represent sample sizes (number of values of daily PAR) for the 2007 monthly averages, and pink numbers represent sample sizes for the 2008 monthly averages. (P1 = PAR1; P2 = PAR2). Note the small sample sizes for the August 2008 averages.

The simulated submarine PAR results for Friday Harbor are shown in Figure 3-7. While there are intervals with apparent differences between the years (e.g. lower July PAR in 2007), there is high variability within each year, and in the difference between the years. The monthly means of the simulated daily PAR at Friday Harbor are shown in Figure 3-8.

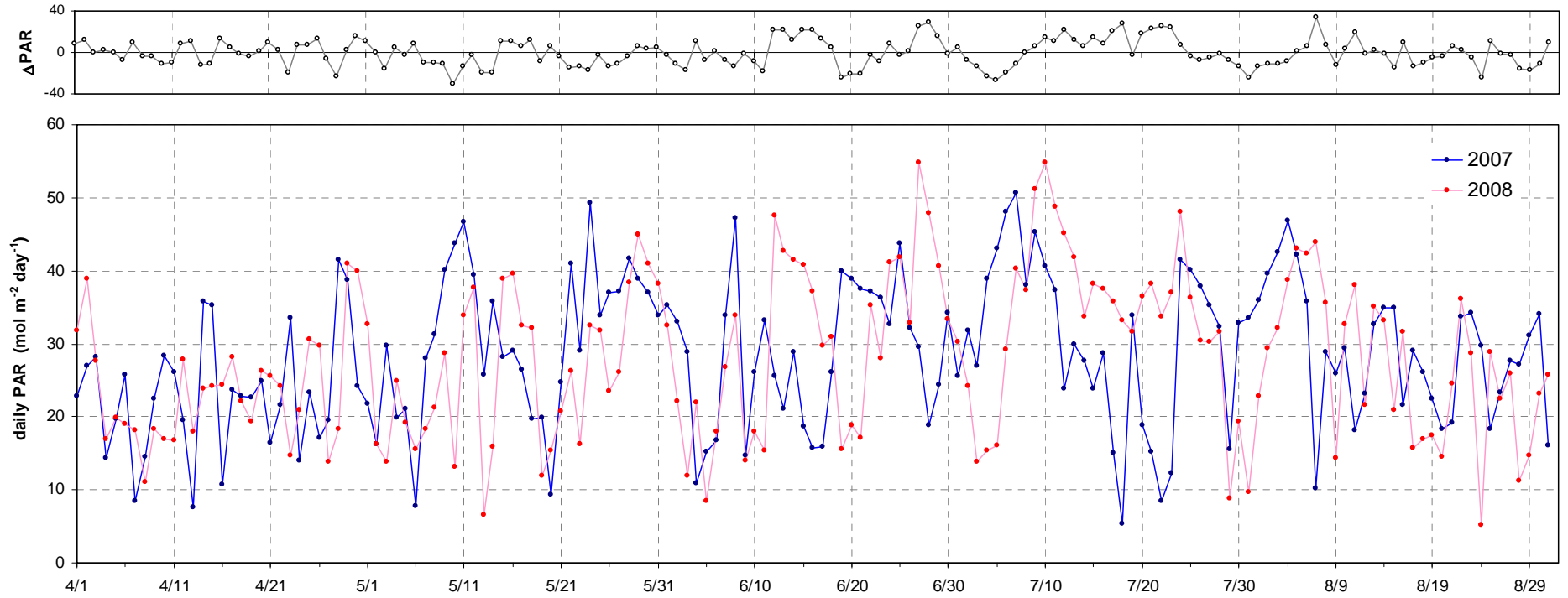


Figure 3-7. Daily PAR simulated for -1.5 m MLLW at Friday Harbor from 4/1 to 8/31. The top graph shows the corresponding PAR difference (2008 minus 2007) between the two years (also in $\text{mol m}^{-2} \text{ s}^{-1}$).

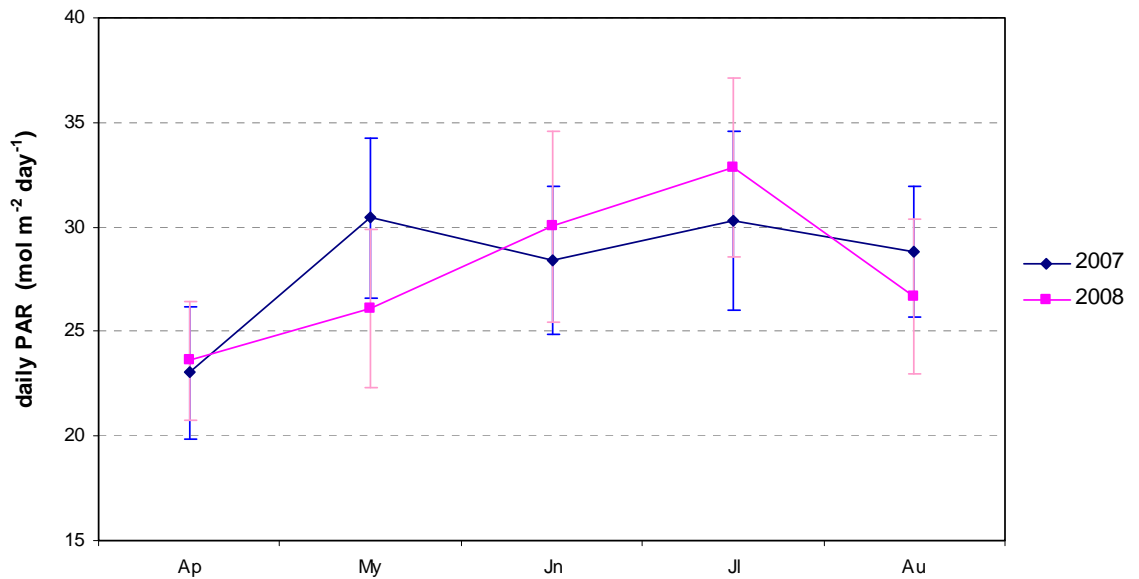


Figure 3-8. Monthly average of daily simulated PAR at -1.5m MLLW depth at Friday Harbor. Error bars are 95% confidence intervals.

The one-way ANOVA with year as the factor did not detect a significant difference between 2007 and 2008 Friday Harbor simulated daily PAR (Table 3-2). The two-way ANOVA with year and month as factors supported the following points (Table 3-3):

- There is significant variation in daily PAR by month.
- There is no significant difference between years.
- There is no significant interaction. This means that the same month effect is seen in both years.

Source of Variation	SS	df	MS	F	P-value
Between Groups	9.699709	1	9.699709	0.088764	0.765958
Within Groups	33219.83	304	109.2758		

Table 3-2. One-way ANOVA table testing for significant difference ($\alpha=0.05$) between 2007 and 2008 simulated daily PAR at Friday Harbor.

Source of Variation	SS	df	MS	F	P-value
Months	2317.388	4	579.347	5.672371	0.000208
Year	6.649575	1	6.649575	0.065106	0.798782
Interaction	636.1064	4	159.0266	1.557025	0.185868
Within	29619.12	290	102.1349		

Table 3-3. Two-way ANOVA table testing for significant effects ($\alpha=0.05$) by month and by year, and for significant interactions between the two, in simulated daily PAR at Friday Harbor.

3.2.2 Comparison of Daily PAR between Stations

The ANOVA that tested for significant differences in mean daily PAR between years (Table 3-1, p.16), included station as a second factor. The differences between stations were found to be very significant. An additional ANOVA is presented here that focuses only on differences between stations. This test benefits from greater accuracy since input data is limited to only days with contemporaneous data across all three stations. Furthermore, the two years are pooled, increasing sample sizes, and for each day, the data from the three stations are “paired” in a repeated measures design. The results confirm that differences between stations are highly significant (Table 3-4).

	Source of Variation	SS	df	MS	F	P-value
PAR1 ANOVA	Day	18273.78	86	212.4858	46.1451	0.000000
	Station	396.8206	2	198.4103	43.08836	0.000000
	Error	792.0138	172	4.604732		
PAR2 ANOVA	Day	10917.15	127	85.961807	22.12952	0.000000
	Station	636.3375	2	318.16877	81.90757	0.000000
	Error	986.6593	254	3.8844854		

Table 3-4. Repeated measures ANOVA tables testing for significant differences ($\alpha=0.05$) between stations in average daily PAR. All days (2007 and 2008) with contemporaneous data across the three stations were included in the analyses. These ANOVAs were run as two-way ANOVAs without replication with day and station as factors

The ANOVAs were followed up with Tukey tests to determine which specific station differences were significant (Zar 1999, p.210). These results show that all stations were significantly different in terms of daily PAR as measured by the PAR1 sensors. As measured by the PAR2 sensors, the head of the bay (WBS and WBN) was significantly different, but WP and BP could not be distinguished. The 2007-2008 average daily PAR values are shown in Figure 3-9.

Station comparison	PAR1 results	PAR2 results
WP vs WBS/WBN	Reject H_0	Reject H_0
BP vs. WBS/WBN	Reject H_0	Reject H_0
WP vs BP	Reject H_0	Accept H_0

Table 3-5. Results of Tukey mulicomparison tests in follow-up to the significant ANOVA results (Table 3-4). In each case, the null hypothesis tested, H_0 , states that average daily PAR was equivalent at the two stations tested. All tests performed at $\alpha=0.05$.

It is important to note that these results are based on the assumption of identical instrument deployment depths at each station. During data analysis, it became clear that there were depth discrepancies that could affect a comparison of PAR across stations. It is not possible to accurately correct for the depth discrepancies with the available information. However, a rough assessment of the effects of the

depth discrepancies on the PAR results is given in Appendix section A.1 (p.44). This assessment suggests that PAR may have been underestimated at WP. Furthermore, the significant difference between average daily PAR at WP and BP measured by the PAR1 sensors (Table 3-5), may be an artifact of the differences in deployment depth.

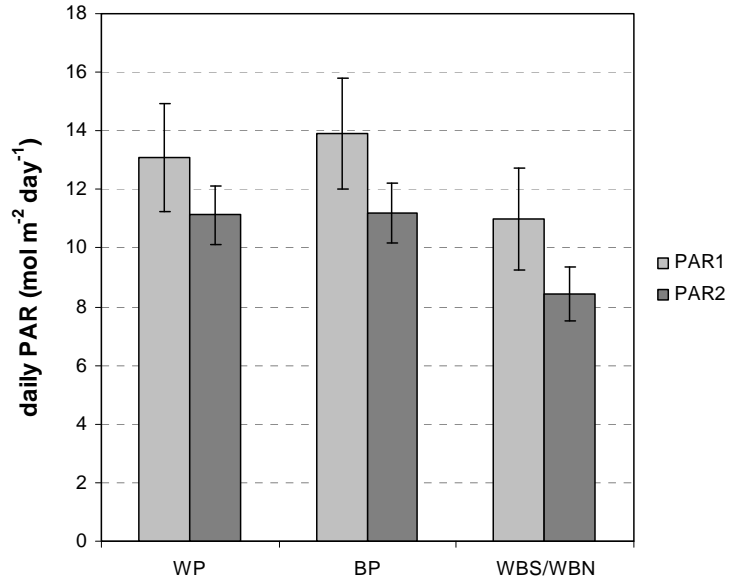


Figure 3-9. Average 2007-2008 daily PAR for the Westcott Bay stations for each PAR sensor. Only days with contemporaneous data across the stations were included in the averages ($n_{PAR1} = 87$; $n_{PAR2} = 129$). Error bars are 95% confidence intervals.

Cumulative daily PAR provides an alternate approach to reducing the daily PAR data for simple station comparisons. Figure 3-10 shows the cumulative PAR separately for data from PAR1 and PAR2 sensors, based on contemporaneous data across the three stations. In both cases, the seasonal cumulative PAR at the head of the bay (WBS/WBN) is substantially lower than WP and BP. Based on the PAR1 data, the seasonal cumulative PAR at the head of the bay was reduced in both years by 17% relative to the next station (WP for both years). Based on the PAR2 data, cumulative PAR at the head of the bay was reduced by 27% in 2007 (WBS) and 23% in 2008 (WBN) relative to the next station (also WP).

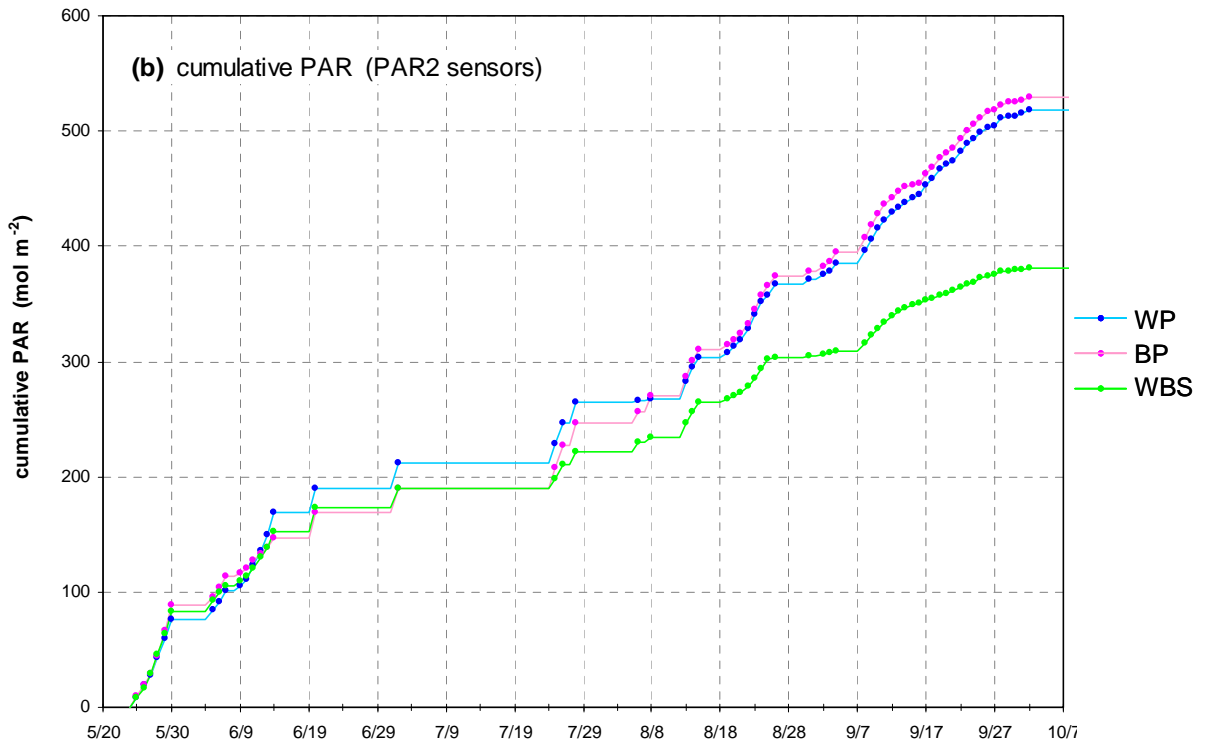
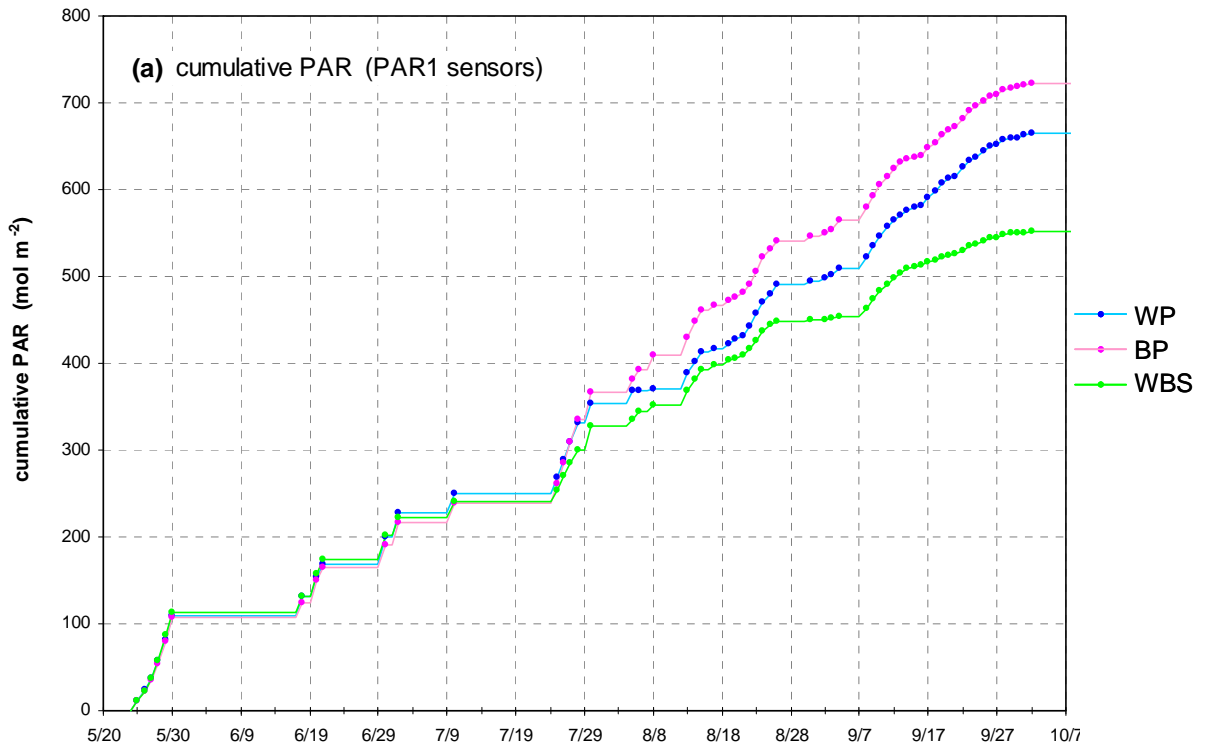


Figure 3-10. 2007 cumulative daily PAR based only on contemporaneous daily PAR estimates at the three stations.

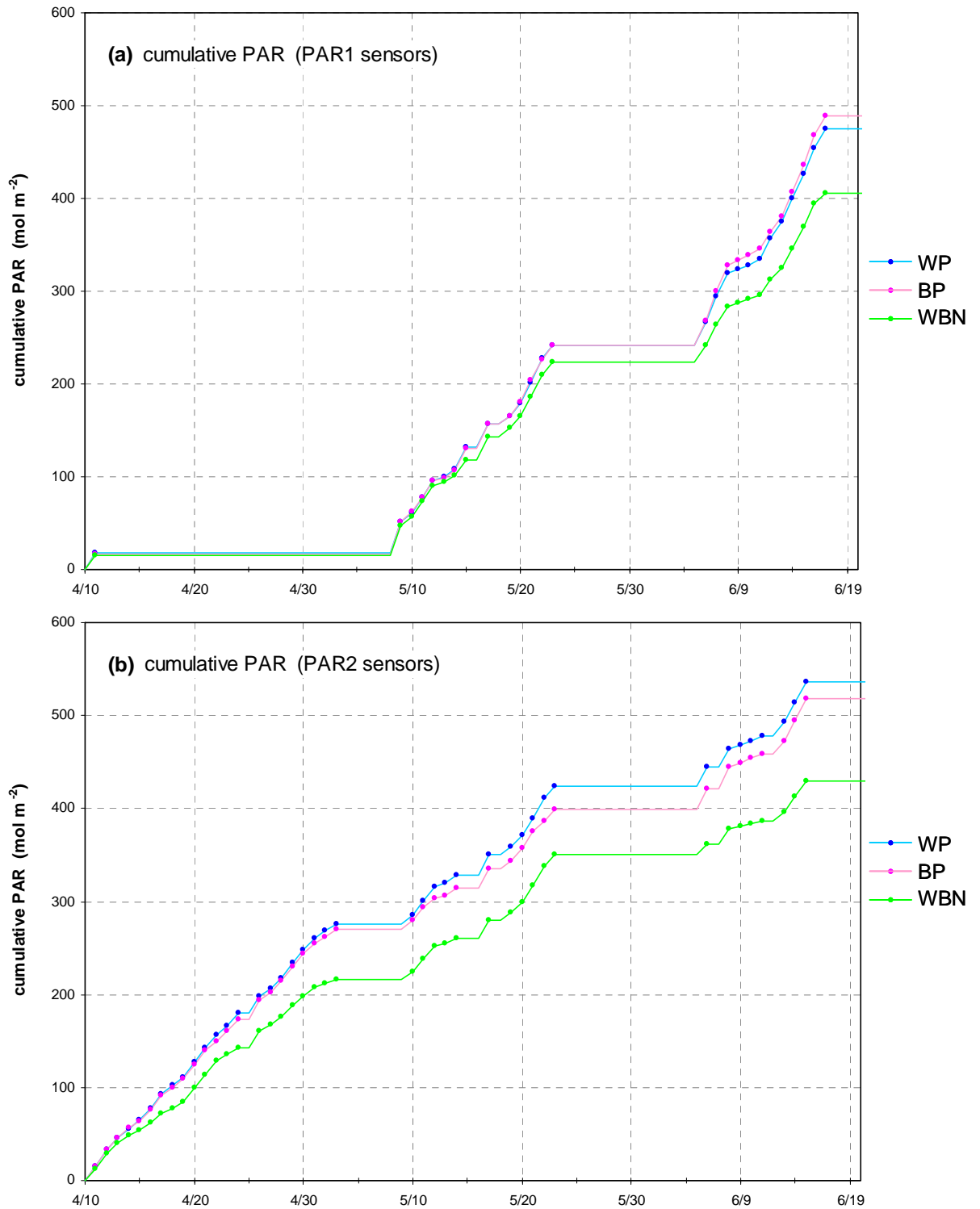


Figure 3-11. 2008 cumulative daily PAR based only on contemporaneous daily PAR estimates at the three stations.

3.3 Attenuation

The daily attenuation time series are shown in Figure 3-12. The high values at BP in 2008 are likely due to bad PAR2 data that was not identified by the cleanup algorithm. Figure 3-13 gives an example of suspicious PAR2 associated with one of these spikes in daily attenuation. Five data points shown with high values were removed from the dataset and not included in the following analyses.

3.3.1 Comparison of Daily Attenuation between Years and between Months

A comparison of the 2007 and 2008 season means of daily attenuation are shown in Figure 3-14. There is no obvious difference between the years. The estimate for BP is greater in 2008, but the estimate for WP is lower in 2008 and there is virtually no difference between years at WBS/WBN. This is supported by the two-way ANOVA results which show that year is not a significant factor ($\alpha = 0.05$), while station is a significant factor. These estimates could reflect a slight bias associated with seasonality since they are based on different distributions of data through the common sampling period of April 21 to August 8 (see Figure 3-5, p.16).

Source of Variation	SS	df	MS	F	P-value
Year	0.0014	1	0.0014	0.022	0.882460
Station	7.0973	2	3.5487	54.449	0.000000
Interaction	0.3151	2	0.1575	2.417	0.090278
Within	31.0226	476	0.0652		

Table 3-6. ANOVA results testing for significant differences in mean daily attenuation between years and between stations.

Estimates of monthly mean attenuation are shown in Figure 3-15. These values were calculated as the arithmetic mean of all daily attenuation values for each month for each station. Comparisons across years are difficult because of the incomplete monthly data series, but two patterns are consistent across plots in Figure 3-15:

- Estimates of May attenuation were greater in 2007 than 2008 across all three stations, although these differences have not been formally tested and the significance of the BP difference is in doubt.
- Estimates of June and July attenuation were lower in 2007 than 2008 at BP and the head of the bay (WBS / WBN). Missing data prevented this comparison at WP.

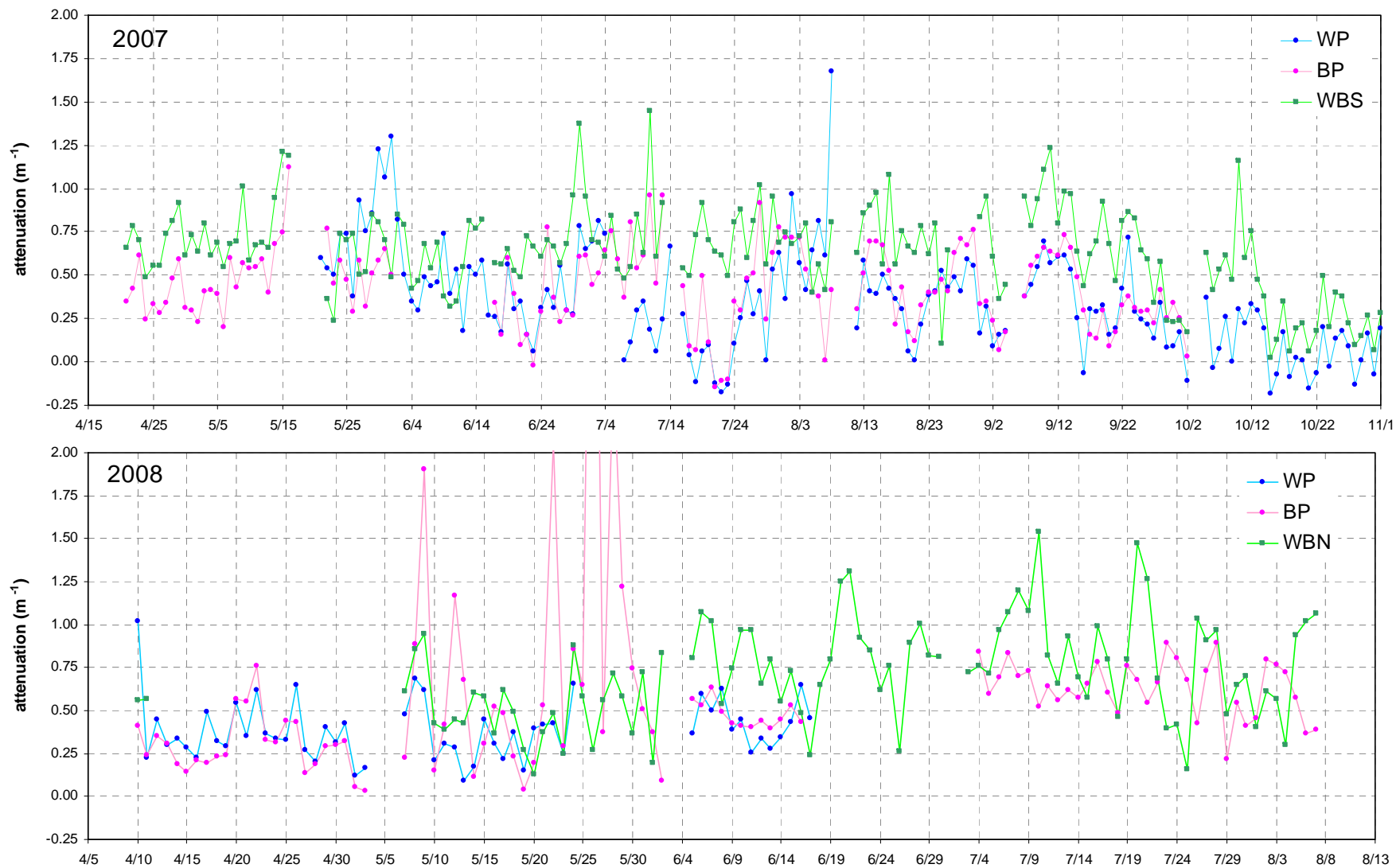


Figure 3-12. 2007 (top) and 2008 (bottom) daily attenuation coefficient.

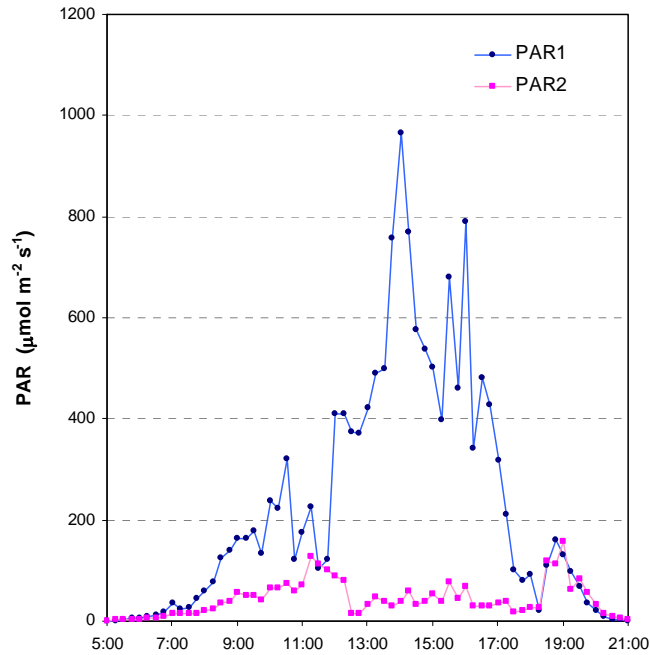


Figure 3-13. PAR data from 26 May 2008. The daily attenuation coefficient based on these data is $k=5 \text{ m}^{-1}$, and is off the chart shown in Figure 3-12. The PAR2 data suggests that that sensor was obstructed, resulting in unreliable PAR data and daily attenuation estimate.

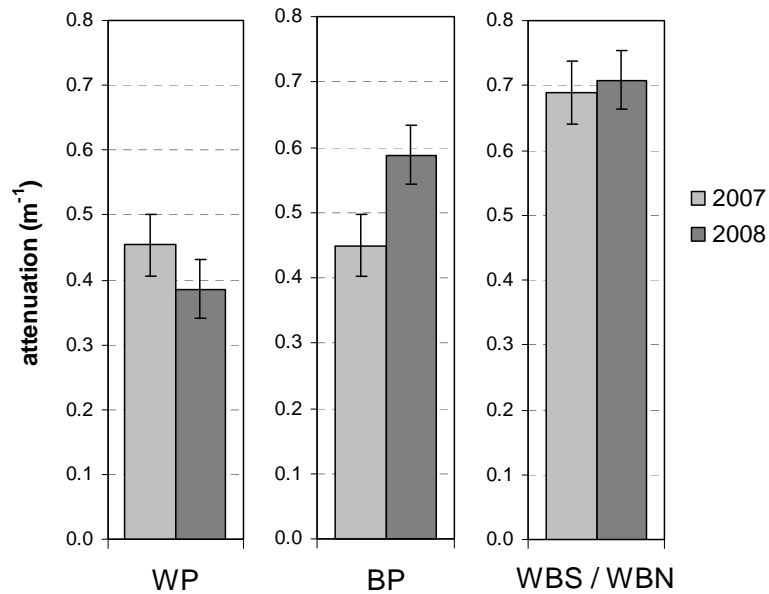


Figure 3-14. Comparison of average daily attenuation coefficients calculated for 2007 and 2008. Daily attenuation values were averaged only over the period that was sampled in both years (April 21 – August 8). Error bars are 95% confidence intervals. The sample sizes for these six averages range from 55 to 102 daily attenuation values. These represent the same data that were tested in the ANOVA in Table 3-6, that showed that the station has a significant effect on the averages. The year did not have a significant effect.

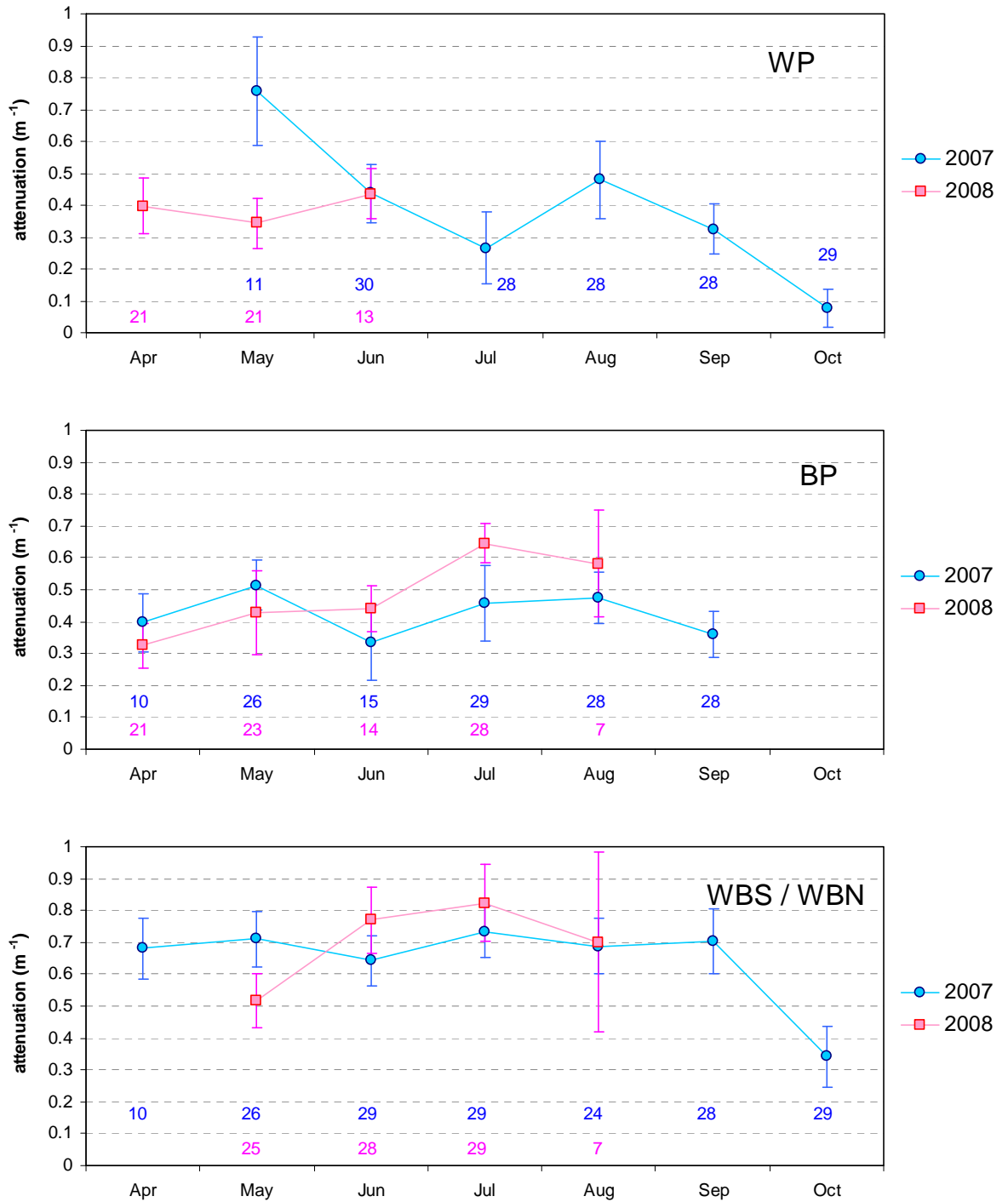


Figure 3-15. Mean monthly attenuation calculated as the arithmetic mean of all available daily attenuation values. Error bars are 95% confidence intervals on the means. Blue numbers represent sample sizes (number of values of daily attenuation) for the 2007 monthly averages, and pink numbers represent samples sizes for the 2008 monthly averages. Note the small sample sizes for the August 2008 averages.

3.3.2 Comparison of Daily Attenuation between Stations

The ANOVA that tested for significant differences in mean daily attenuation between years (Table 3-6, p.24) included station as a second factor. The differences between stations were found to be very significant. An additional ANOVA is presented here that focuses only on differences between stations. This test benefits from greater accuracy since input data is limited to only days with contemporaneous data across all three stations. Furthermore, the two years are pooled, increasing sample sizes, and for each day, the data from the three stations are “paired” in a repeated measures design. The results confirm that differences between stations are highly significant (Table 3-7).

<i>Source of Variation</i>	<i>SS</i>	<i>df</i>	<i>MS</i>	<i>F</i>	<i>P-value</i>
Day	16.979	137	0.123934	2.370429	0.000000
Station	6.136467	2	3.068233	58.68456	0.000000
Error	14.32567	274	0.052283		

Table 3-7. Repeated measures ANOVA tables testing for significant differences ($\alpha=0.05$) between stations in average daily attenuation. All days (2007 and 2008) with contemporaneous data across the three stations were included in the analyses.

The ANOVA was followed up with Tukey’s test to determine which specific station differences were significant (Zar 1999, p.210). These results show that all stations were significantly different in terms of average daily attenuation (Table 3-8). The 2007-2008 average daily attenuation values are shown in Figure 3-16.

Station comparison	Attenuation results
WP vs WBS/WBN	Reject H_0
BP vs. WBS/WBN	Reject H_0
WP vs BP	Reject H_0

Table 3-8. Results of Tukey mulicomparison tests in follow-up to the significant ANOVA results (Table 3-7). In each case, the null hypothesis tested, H_0 , states that average daily attenuation was equivalent at the two stations tested. All tests performed at $\alpha=0.05$.

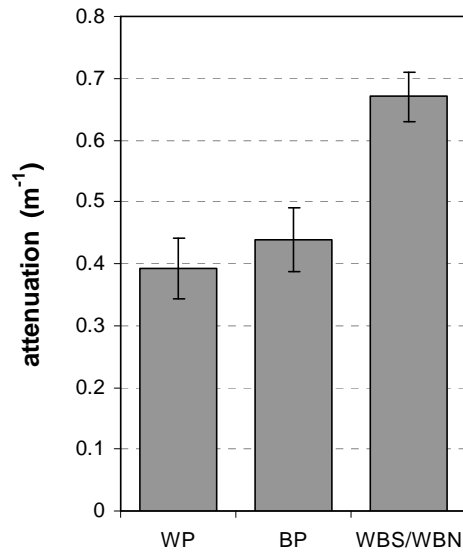


Figure 3-16. Average 2007-2008 daily attenuation. Only days with contemporaneous data across the stations were included in the averages ($n=138$ days). Error bars are 95% confidence intervals. The average attenuation for each station is significantly different than the others (Table 3-8).



4 Discussion

The PAR results are supported by the attenuation results, and they both lead to the following characterization of PAR across the Westcott Bay stations (Table 4-1):

- Average levels of PAR at the head of the bay (WBS / WBN) are reduced relative to other areas of the bay (both BP and WP stations). The magnitude of this reduction is roughly 20% as measured by mean daily PAR and cumulative PAR. Average water column attenuation is increased at the head of the bay.
- Average levels of PAR at BP and WP are very similar. Average attenuation is very similar between BP and WP.

	WP	BP	WBS / WBN
Average daily PAR (mol m ⁻² day ⁻¹) (PAR2 sensor; Figure 3-9, p.21; compare to depth-adjusted results in Figure A-8, p.52)	11.1 ± 1.0	11.2 ± 1.0	8.4 ± 0.9 *
Average attenuation (m ⁻¹) (Figure 3-16, p.29)	0.39 ± 0.05*	0.44 ± 0.05*	0.67 ± 0.04 *

Table 4-1. Summary of average 2007-2008 PAR and attenuation results (* = significantly different from other stations, α=0.05).

The PAR and attenuation parameters are subject to different limitations. The PAR parameters provide the most direct measure of the environmental variable of interest – levels of PAR that would be available to an eelgrass plant at a given location. However, measurements of PAR are very sensitive to depth of deployment. Therefore, the strength of comparisons of PAR across stations rests on tight control of instrument deployment depth. It is very difficult to control deployment depth to within centimeters in a soft sediment nearshore environment. An analysis of depth data across the stations in this study showed that depth discrepancies were large enough to compromise the ability to discriminate between stations with similar PAR results (WP and BP; Appendix A.1).

In contrast, attenuation results are relatively insensitive to modest differences in deployment depth since attenuation is based on the difference in readings between two sensors with a fixed height difference. Where deployment depth problems are suspected, it is useful to consider attenuation results for this reason. However, attenuation is only indirectly related to the environmental variable of interest (PAR

incident on eelgrass leaves). Furthermore, attenuation was measured over only a portion of the water column (40 vertical cm) which, depending on vertical structure, may be a poor representation of the entire water column.

The fact that both the PAR results and the attenuation results are consistent increases our confidence in the overall characterization. We can now revisit our initial hypotheses.

4.1 Does PAR Availability Match the Pattern of Eelgrass Loss?

Let us start with the finding that PAR is reduced at the head of the bay where eelgrass has completely disappeared. By itself, this suggests that the pattern of available PAR matches the pattern of eelgrass loss. However, when we also consider the findings at BP, this relationship no longer holds.

BP can be considered to be an intermediate location in terms of current eelgrass abundance because there is a small, residual sub-tidal bed north of the YSI station and to the south there is some surviving eelgrass, albeit very sparse (Figure 4-3). But in general the eelgrass abundance is very low and this station is more similar to the head of the bay than to WP in terms of current eelgrass condition. During the fieldwork there was no eelgrass in the immediate vicinity of the BP YSI instrument, and only one plant was observed in an area of at roughly 200 m² around the instrument. Furthermore, when put in a longer temporal context, the Bell Point area in general must be placed in a category of extreme eelgrass loss. Extensive beds in the intertidal and subtidal have been lost (Figure 4-1).



Figure 4-1. 2003 photo from the east side of Bell Point looking west. Extensive eelgrass is visible throughout the foreground up to the lower zone of the exposed shoreline in the background. Eelgrass has completely disappeared from these areas. The residual subtidal bed would be underwater to the right of the exposed point.

The fact that BP and WP have essentially indistinguishable levels of PAR, but very different levels of current eelgrass abundance (as well as recent trajectories in abundance), leaves us unable to reject the null hypothesis presented on page 4:

H_{01} : There is no difference in PAR availability between areas that have lost eelgrass and areas that currently sustain eelgrass in Westcott Bay.

The lack of a relationship between PAR and eelgrass abundance is shown in Figure 4-2. Clearly, if only WP and WBS/WBN were compared, a different conclusion would be reached – i.e. PAR would seem to predict eelgrass abundance. It is essentially the BP data point that precludes us from rejecting the null hypothesis.



Figure 4-2. Conceptual representation of the three stations placed in a space of eelgrass survival and PAR availability. Under the hypothesis of low PAR-induced eelgrass loss, prior to 2003 all stations were in the position of WP – i.e. intact eelgrass with high levels of PAR. The arrows represent trajectories over time as WBS/WBN and BP experienced extreme loss of eelgrass. PAR does not explain the change in eelgrass survival in these two trajectories, undermining this hypothesis.

This conclusion is vulnerable to an argument that different stressors may be acting at different locations in the Westcott Bay area. The analysis would then be confounded by considering all three stations as representing a single population. This may be true to some extent, but when the area is considered more synoptically it seems reasonable to assume there is some shared mechanism behind the loss of eelgrass across Westcott and Garrison bays. Figure 4-3 shows that eelgrass loss is complete across the inner bays and persists only in close proximity to the mouth at Mosquito Pass. Although not shown, eelgrass persists and is abundant at the mouth and outside the bay in areas of Mosquito Pass. While not definitive, the

concentration and the extensive nature of the losses in these enclosed embayments suggest there is some shared causal mechanism.

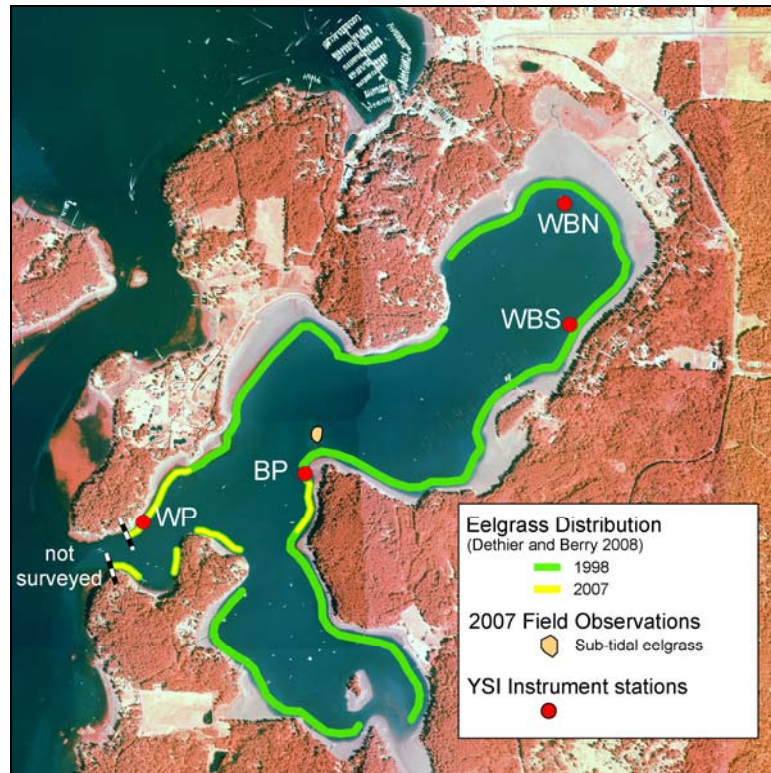


Figure 4-3. Changes in the distribution of eelgrass in the Westcott Bay area (Dethier and Berry 2008). Field observations of the Bell Point subtidal bed made by snorkeling are also shown (Zach Hughes and Kevin Britton-Simmons, UW Friday Harbor Labs).

4.2 Do Differences between Stations have Physiological Significance?

It is unknown, but certainly plausible, that the roughly 20% reduction in PAR at the head of the bay would be large enough to have some measurable plant response. However, such an effect would not necessarily take the form of lowered productivity. Lee et al. (2007) emphasize the ability of plants to acclimate to local light conditions – even to the extent that productivity may not change proportionally with local light conditions. Theoretically, such adaptation could be detected through assessment of leaf-level photosynthesis.

The second hypothesis presented on p.4 is narrow in scope, and therefore does not definitively address the question of physiological significance of observed PAR differences. But it does serve as a starting point for evaluating the potential significance of the lowered average PAR observed at the head of the bay:

H_{02} : PAR levels in areas of eelgrass loss are greater or equal to the minimum PAR requirements reported in the literature for other sites.

In the course of this study, it became clear that a comparison to literature values is somewhat problematic because of the complexity of defining a minimum light requirement parameter as well as the wide range of reported values for particular parameters (Moore et al 1997). Minimum light requirements are most commonly reported as a percentage of surface irradiance (% SI) (Burd and Dunton 2001; Dennison et al. 1993; Dunton 1994; Kenworthy and Fonseca 1996; Lee et al. 2007; Lee and Dunton 1997; Longstaff and Dennison 1999; Steward et al. 2005), or as the number of hours with saturating PAR irradiance, H_{sat} (Dennison and Alberte 1985; Dunton 1994; Herzka and Dunton 1988; Zimmerman et al. 1991). The underwater PAR measurements from Westcott Bay were not accompanied by measurements of surface irradiance, so it is not possible to make direct comparisons to light requirements reported as % SI. It would be possible to make H_{sat} estimates using estimates of saturating PAR from Selting et al. (2007), and there is an opportunity for future analysis on this topic.

The most valuable estimate of minimum light requirements for this study is presented by Thom et al. (2008). They report minimum light requirements in terms of average daily PAR based on measurements with eelgrass beds in the Pacific Northwest of the US. According to their assessment, the minimum level of average daily PAR through the spring and summer that is required for eelgrass survival is $3 \text{ mol m}^{-2} \text{ day}^{-1}$. Moore et al (1997) also report that *Z. marina* transplants died after 30 days of exposure to light levels below $3 \text{ mol m}^{-2} \text{ day}^{-1}$.

While the average daily PAR is reduced at the head of Westcott Bay relative to WP and BP, it is still greater than this reported minimum value of $3 \text{ mol m}^{-2} \text{ day}^{-1}$ by almost a factor of three ($8.4 \text{ mol m}^{-2} \text{ day}^{-1}$; Table 4-1, p.30). This WBS/WBN estimate is actually depressed somewhat due to the inclusion of lower PAR data from October, after the spring-summer window used by Thom et al. (2008).

This comparison does not support the rejection of the null hypothesis above. Although this comparison is limited, it suggests that the reduced light at the head of Westcott Bay should be sufficient to support eelgrass survival.

This conclusion is vulnerable to the argument that light requirements are site-specific and dependent on a suite of local environmental parameters. The value reported by Thom et al. (2008) and Moore et al. (1997) may not therefore be appropriate for application in Westcott Bay. Light requirements could conceivably be elevated at a site that has relatively high plant respiration rates or high primary production requirements to counteract herbivory or combat disease. In such a case, relatively high PAR levels could still be considered a co-limiting stressor in concert with other stressors.

This possibility cannot be dismissed at the head of the bay, but two considerations argue against its importance. First, the large difference between average daily PAR at the head of the bay and the published minimum makes this seem unlikely. The

value at the head of the bay is nearly threefold greater ($8.4 \text{ mol m}^{-2} \text{ day}^{-1}$) than the minimum. This would leave a substantial amount of PAR available to cover any elevated primary production requirements before net PAR is reduced below the minimum requirement observed in other Pacific Northwest eelgrass beds.

The second consideration focuses on the pattern of eelgrass abundance at Bell Point. This consideration suggests that in addition to not being the primary causal factor for eelgrass loss there, reduced PAR is not even an important co-limiting stressor. Prior to this study, it was known that scattered eelgrass plants persisted around Bell Point. During the 2007 field work, a discrete subtidal bed off Bell Point was delineated (Figure 4-3). Given the extensive loss of eelgrass at higher tidal elevations at Bell Point, this suggests that there has been preferential survival at depth in a zone of greater light limitation. This is not consistent with reduced PAR as even a co-limiting stressor.

Bell Point is a unique geomorphological feature within the Westcott Bay area, and likely has a unique tidal current and energy environment. Nevertheless, when considering the extensive pattern of eelgrass loss in Westcott and Garrison Bays, including Bell Point (Figure 4-3), it seems more likely that another unidentified stressor is playing a key role in this system, rather than reduced PAR plays a key role elsewhere within the Westcott system but not at Bell Point. Given that the currents and energy are likely unique at Bell Point, there also may be unique substrate characteristics. The sediment maps of Grossman et al. (2007) suggest this may be the case. Exploring other parameters such as these may be more fruitful for explaining the persistence of a subtidal eelgrass bed at Bell Point.

4.3 Lessons Learned – PAR Data from the YSI 6600 EDS Platform

The study described in this report represents a first effort by the Nearshore Habitat Program in deploying unattended PAR sensors and a first experience specifically with the YSI 6600 EDS. Beyond the ecological significance of the results, there were two broad lessons learned.

First, significant instrument issues may be present. Distinct patterns of errors were identified in the data used in this study (Figure B-1, p.68). The issue of signal loss has been addressed with YSI. Since the end of 2008 sampling, YSI found a problem with the instrument electronics and many cases of malfunctioning PAR wipers were observed – in some cases leading to significant loss of data (Figure 3-1, p.12). YSI has serviced all DNR's instrument electronics and PAR wiper motors to remedy this problem. This experience emphasizes the need to regularly (at least annually) perform instrument intercomparisons and, ideally, perform in-water testing. Particular attention should be paid to these problems to ensure they have been eliminated.

The second overall lesson was that the development and application of cleanup and analysis procedures for these datasets is enormously time consuming when

performed at this level of detail. The project will likely realize major efficiencies with continued deployments, but the cleanup and analysis will still require substantial effort. It is important to fully consider this effort when planning research activities. To be most effective, deployments need to be designed to be tightly linked to specific research questions. This will ensure that the scope of the deployment is appropriate and help guide data processing and analysis.

Over the longer term, DNR should consider developing tools on a new development platform such as R. Currently, processing is increasingly efficient as new data is processed, but virtually all analysis takes place within Microsoft Excel and there will always be extensive user involvement required. A migration to R would require training of a developer to create analysis tools, but training of users would be minimal and probably significantly less than training on the entire processing chain within Excel.

Also, given that research questions may require only a subset of the parameters collected by the YSI instruments, and the limited in-house processing capacity, DNR should actively encourage data analysis by other researchers and streamline data distribution. Either raw or minimally processed data could be distributed over the internet or through academic contacts. This would be service to the scientific community and could entice an increase in processing capacity to focus on issues of interest to DNR.



5 Summary and Recommendations

This report describes the deployment of YSI continuous water quality monitoring instruments in Westcott Bay on San Juan Island, Washington, from 4/22/07 to 11/2/07. The instruments were deployed at three stations from the mouth to the head of the bay that coincides with a gradient in severity of *Z. marina* decline. There has been total loss at the head of the bay (WBS), substantial loss at Bell Point (BP) and presumably little or no loss at White Point (WP) near the mouth of the bay – currently the station with the largest and apparently healthiest *Z. marina* population. This work was initiated to help explain the causes of this *Z. marina* decline. This report includes details of the PAR data cleanup procedures that were developed, and the analysis of differences in PAR availability and water column attenuation between the three stations.

Key findings include:

- PAR and attenuation observations indicate that PAR at the head of the bay is reduced relative to other points in the Westcott Bay area. In terms of mean daily PAR and season cumulative PAR, this reduction at the head of the bay is roughly 20%.
- The reduced average daily PAR at the head of the bay ($8.4 \text{ mol m}^{-2} \text{ day}^{-1}$) is still nearly threefold greater than the minimum requirements for eelgrass survival reported for eelgrass beds in Pacific Northwest estuaries ($3 \text{ mol m}^{-2} \text{ day}^{-1}$; Thom et al., 2008).
- Average daily PAR was indistinguishable between the mouth of the bay (WP) and Bell Point (BP). Average attenuation was also very similar.

The stark differences in eelgrass abundance and survival between the mouth of bay (WP; high abundance) and Bell Point (BP, low abundance), do not correspond with the finding that these stations have indistinguishable available PAR. This suggests that PAR is not an important controlling factor on eelgrass abundance in the Westcott Bay area.

Furthermore, the pattern of eelgrass loss at Bell Point suggests that low PAR is not even an important co-limiting factor in determining eelgrass survival. The fact that Bell Point does have a discrete, residual bed in the subtidal presents a unique opportunity for isolating key stressors. This eelgrass bed has high conservation

value due to its rarity in the Westcott area, and any work here must bear this in mind, but it should be a focus of future research.

This was the first effort by the Nearshore Habitat Program to deploy unattended PAR sensors and analyze the resultant datasets. It is now clear that the development of data cleanup and analysis procedures for these datasets is a large effort that cannot feasibly be replicated for all sensors deployed on an ongoing operational basis. Analysis procedures should be further standardized so they can be applied in a more automated fashion without further development. This could be greatly advanced with migration to an analysis platform such as R. Deployments need to be designed to be tightly linked to specific research questions. This will maximize the efficiency of deployments and guide data processing and analysis.

Recommendations for future instrument deployments:

- Conduct regular instrument intercomparisons to identify instrument and deployment problems.
- Develop processing and analysis tools on a platform that is compatible with automated usage in a more operational context (e.g. R, but also Matlab/Octave).
- Deployments should be restricted to cases where (a) they are driven by specific research questions that require the data or (b) they are added onto other intensive field efforts (e.g. transplant experiments) with only modest additional effort.
- Consistently record instrument conditions (fouling, wiper operation) at each retrieval.
- Make the complete YSI datasets available to other researchers either over the internet or through academic contacts. This may allow additional data to be analyzed that are not a DNR priority, and may increase interest in research questions of interest to DNR.

Research Priorities for Westcott Bay

This study identified a new research priority for the Eelgrass Stressor-Response Project in resolving the causes of eelgrass decline in Westcott Bay. There are additional research priorities associated with the 2007-2008 data collection that logically follow the analysis of PAR data presented in this report. These priorities should be balanced with others being considered within the broader objectives of the Eelgrass Stressor-Response Project.

- Develop hypotheses and field experiments that focus on the Bell Point subtidal eelgrass bed and the factors that have led to its persistence but also its contraction to a small residual bed.
- Further analyze data collected in the 2007-2008 study by other sensors on the YSI instruments at the Westcott Bay stations.
 - Analyze the temperature data for differences between stations and interannual differences. Findings should be considered in the context of

Pacific Northwest climate variability, particularly the patterns of El Niño and Pacific Decadal Oscillation indices.

- Analyze the chlorophyll and turbidity data to characterize phytoplankton dynamics and sediment resuspension.
- Generate gross summaries of the dissolved oxygen, salinity and pH.



6 References

- Burd, A.B. and K.H. Dunton, 2001, Field verification of a light-driven model of biomass changes in the seagrass *Halodule wrightii*, **Marine Ecology Progress Series**, 209:85-98.
- Carruthers, T.J.B., B.J. Longstaff, W.C. Dennison, E.G. Abal, K. Aioi, 2001, Measurement of light penetration in relation to seagrass, In: Short, F.T. and R.G. Coles (eds.) **Global Seagrass Research Methods**, Elsevier, Amsterdam, pp.369-392.
- Dennison, W.C., R.J. Orth, K. A. Moore, J. Court Stevenson, V. Carter, S. Kollar, P.W. Bergstrom and R.A. Batiuk, 1993, Assessing Water Quality with Submersed Aquatic Vegetation, **BioScience**, 43(2):86-94.
- Dennison and Alberte, 1985, Role of daily light period in the depth distribution of *Zostera marina* (eelgrass), **Marine Ecology Progress Series**, 25:51-61.
- Dethier, Megan N. and Helen D. Berry, 2008, Decadal Changes in Shoreline Biota in Westcott and Garrison Bays, San Juan County, Washington State Department of Natural Resources, Olympia WA.
- Dowty, P., A. Schanz and H. Berry (eds.), 2007, **Eelgrass Stressor – Response Project: 2005-2007 Report**, Nearshore Habitat Program, Washington Department of Natural Resources, Olympia WA. Available online: http://www.dnr.wa.gov/Publications/aqr/nrsh_05_07_biennial_report.pdf
- Dunton, 1994, Seasonal growth and biomass of the subtropical seagrass *Halodule wrightii* in relation to continuous measurements of underwater irradiance, **Marine Biology**, 120:479-489
- Gaeckle J., P. Dowty, B. Reeves, H. Berry, S. Wyllie-Echeverria, and T. Mumford, 2007, **Puget Sound Submerged Vegetation Monitoring Project: 2005 Monitoring Report**, Nearshore Habitat Program, Washington Department of Natural Resources, Olympia WA. Available online: http://www.dnr.wa.gov/Publications/aqr/nrsh_2005_svmp_report.pdf
- Grossman, E., A. Stevens, C. Curran, C. Smith and A. Schwartz, 2007, Bathymetry, Substrate and Circulation in Westcott Bay, San Juan Islands,

Washington, USGS Open File Report 2007-1305. Accessed 5/16/08 at:
<http://pubs.usgs.gov/of/2007/1305/>

- Herzka, S.Z. and K.H. Dunton, 1998, Light and carbon balance in the seagrass *Thalassia testudinum*: evaluation of current production models, **Marine Biology**, 132:711-721.
- Kenworthy, W.J. and M.S. Fonseca, 1996, Light Requirements of Seagrasses *Halodule wrightii* and *Syringodium filiforme* Derived from the Relationship Between Diffuse Light Attenuation and Maximum Depth Distribution, **Estuaries**, 19(3):740-750
- Kirk, 1977, Use of a quanta meter to measure attenuation and underwater reflectance of photosynthetically active radiation in some inland and coastal southeastern Australian waters, **Australian Journal of Marine and Freshwater Research** 28:9-21.
- Kirk, 1984, Dependence of relationship between inherent and apparent optical properties of water on solar altitude, **Limnology and Oceanography**, 29:350-356.
- Kopp, B.S. and H.A. Neckles, 2004, Development of Protocols for Tracking Nutrient Enrichments to Estuaries: National Park Service Vital Signs Monitoring Program – Virginia to Maine, Poster presented at Patuxent Wildlife Research Center Biennial Science Meeting, February 2004. Available online: <http://www.pwrc.usgs.gov/products/posters2004.cfm>
- Lee, K.-S., S.R. Park and Y.K. Kim, 2007, Effects of irradiance, temperature, and nutrients on growth dynamics of seagrasses: A review, **Journal of Experimental Marine Biology and Ecology**, 350:144-175.
- Lee, K.-S., K.H. Dunton, 1997, Effects of *in situ* light reduction on the maintenance, growth and partitioning of carbon resources in *Thalassia testudinum* Banks ex König, **Journal of Experimental Marine Biology and Ecology**, 210:53-73
- Longstaff, B.J. and W.C. Dennison, 1999, Seagrass survival during pulsed turbidity events: the effects of light deprivation on the seagrasses *Halodule pinifolia* and *Halophila ovalis*, **Aquatic Botany**, 65:105-121.
- Moore, K.A., B. Anderson, J. Campbell, M. Lizotte and B. Neikirk, 2004, Measurement of Downwelling Irradiance and Light Attenuation Using a YSI 6600 Extended Deployment System, Poster presented at Biennial Meeting of Estuarine Research Federation, Seattle, 2004.

-
- Moore, K.A., R.L. Wetzel and R.J. Orth, 1997, Seasonal pulses of turbidity and their relations to eelgrass (*Zostera marina* L.) survival in an estuary, **Journal of Experimental Marine Biology and Ecology**, 215:115-134.
- Steward, J.S., R.W. Virnstein, L.J. Morris and E.F. Lowe, 2005, Setting Seagrass Depth, Coverage, and Light Targets for the Indian River Lagoon System, Florida, **Estuaries**, 28(6):923-935.
- Thom, R.M., S.L. Southward, A.B. Borde and P. Stoltz, 2008, Light Requirements for Growth and survival of Eelgrass (*Zostera marina* L.) in Pacific Northwest (USA) Estuaries, **Estuaries and Coasts**, 31:969-980.
- Wyllie-Echeverria, S. T.F. Mumford, J. Gaydos and S. Buffum, 2003, *Z. marina* declines in San Juan County, WA: Westcott Bay Taskforce Mini-Workshop, 26 July 2003, SeaDoc Society. Accessed 5/16/08 at <http://www.vetmed.ucdavis.edu/whc/seadoc/pdfs/eelgrassrpt.pdf>
- Zar, J.H., 1999, **Biostatistical Analysis**, 4th edition, Prentice-Hall.
- Zimmerman, R.C., J.L. Reguzzoni, S. Wyllie-Echeverria, M. Josselyn and R.S. Alberte, 1991, Assessment of environmental suitability for growth of *Zostera marina* L. (eelgrass) in San Francisco Bay, **Aquatic Botany**, 39:353-366.

Appendices

Appendix A PAR Deployment Issues

A.1 Variation in Deployment Elevation

The intention was to locate each YSI instrument above sediment that was at an elevation of

-1.5m MLLW, and place each instrument so that the lower sensors were 20cm above the sediment surface.

A close comparison of depth observations at WBS/WBN, BP and WP indicated that there are essentially no discernable differences in tidal phase within the limits of data collected at 15 and 30 minutes intervals. This suggests that if the YSI instruments were deployed at exactly the same elevation, there would be no differences in observed depth. Any differences in observed depth could then be attributed to one or more of the following errors (in addition to instrument errors associated with calibration or fouling):

1. Error in the location of the instrument where the sediment surface is at an elevation of -1.5m MLLW. Some error is expected since predicted tides were used with water column depth to locate the instruments. Departures of actual tides from predicted values were not considered. This error would be reflected as a constant offset relative to the other stations and would be present for all deployment periods.
2. Error in vertical placement of the PVC deployment tube so that the distance between a correctly seated instrument and the sediment surface would differ from the target 20cm. Some error is expected because field conditions at installation limited the precision of vertical placement. This error would be reflected as a constant offset relative to the other stations and would be present associated for all deployment periods.
3. Error in seating the instrument so that it was not completely lowered to the stop at the bottom of the PVC deployment tube. This error would presumably vary between deployment periods although a station may have been particularly susceptible to this error due to tightness of fit of the PAR bracket in the PVC deployment tube.

A comparison of depth differences across pairs of stations shows not only that the differences depart from 0, but that there is variation across individual deployments (Figure A-1). The magnitude of these departures reaches a maximum of 15 cm. Another view of this pattern is given in Figure A-3 and Figure A-4, which show time series data of the individual depth difference observations. The erratic pattern in late May in 2007 for the BP-WBS and WP-WBS differences demonstrate that problems with instrument seating in the deployment apparatus occurred. The WBS instrument was retrieved briefly on May 25 and upon re-deployment the instrument did not seat correctly (Figure A-5).

Examination of differences between paired stations shows that there were differences in deployment depths, and that these differences varied between deployments. But it does not definitively show which individual stations experienced depth changes, although some patterns can be deduced, e.g. WP was deployed deeper than the other stations. To address this, a tide series was generated to be used to provide a standard for absolute comparisons. The approach used to generate the tide series is described on page 61.

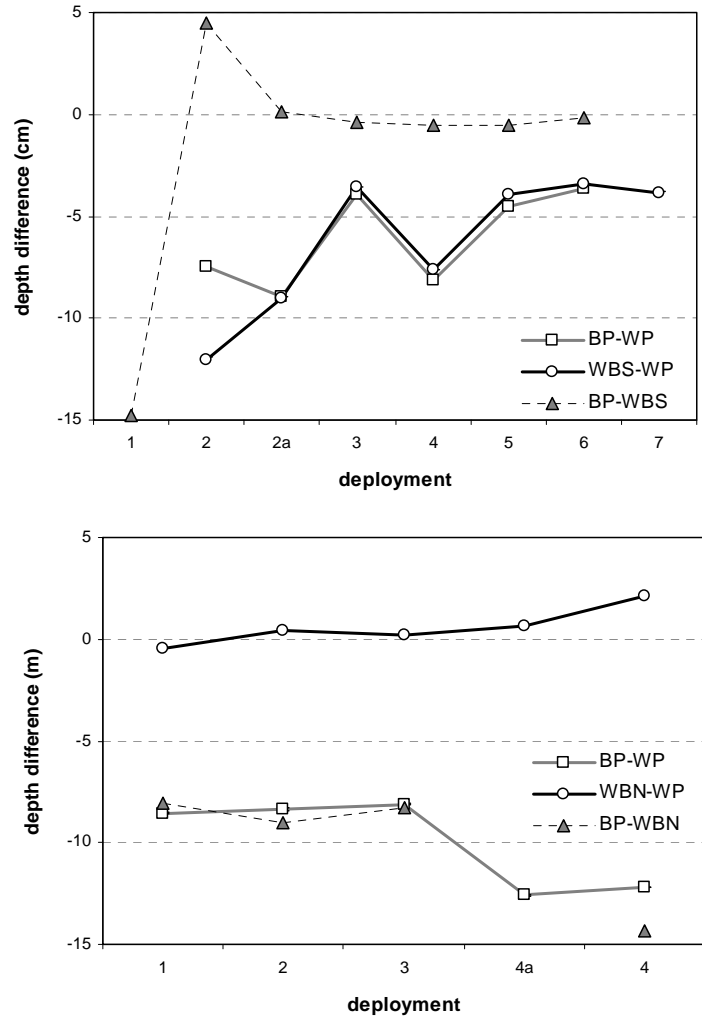


Figure A-1. Depth differences between pairs off stations averaged across each discrete deployment in 2007 (top) and 2008 (bottom). These means are based on a large number of values and the 95% confidence intervals on the means are smaller than the symbols used in these plots.

Differences between depth observations and the estimated tide were used to isolate deployment depth changes at individual stations. Results of this analysis are shown in Figure A-2.

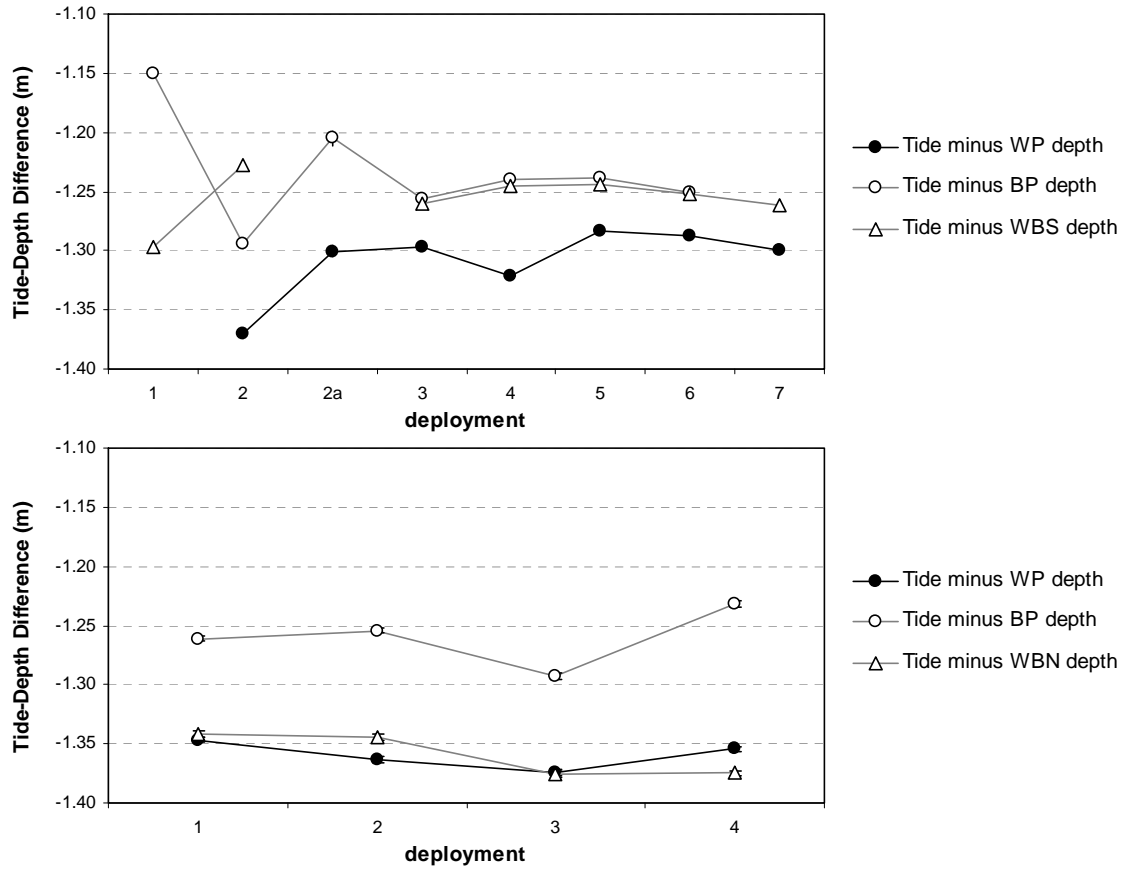


Figure A-2. Mean differences between station depth observations and estimated tide for 2007 (top) and 2008 (bottom). The 95% confidence intervals are smaller than the symbols in the plots.

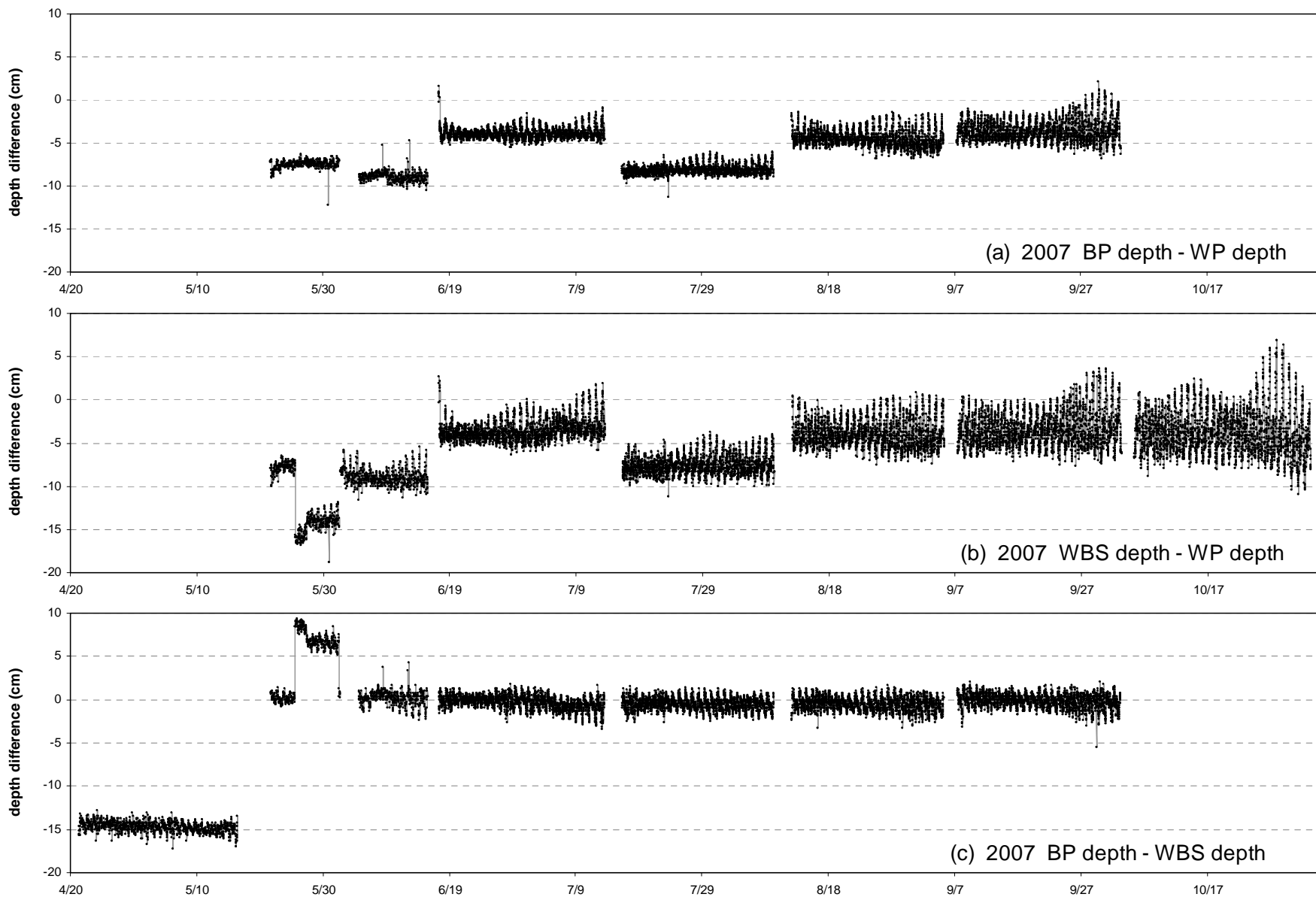


Figure A-3. 2007 time series of depth differences between paired stations.

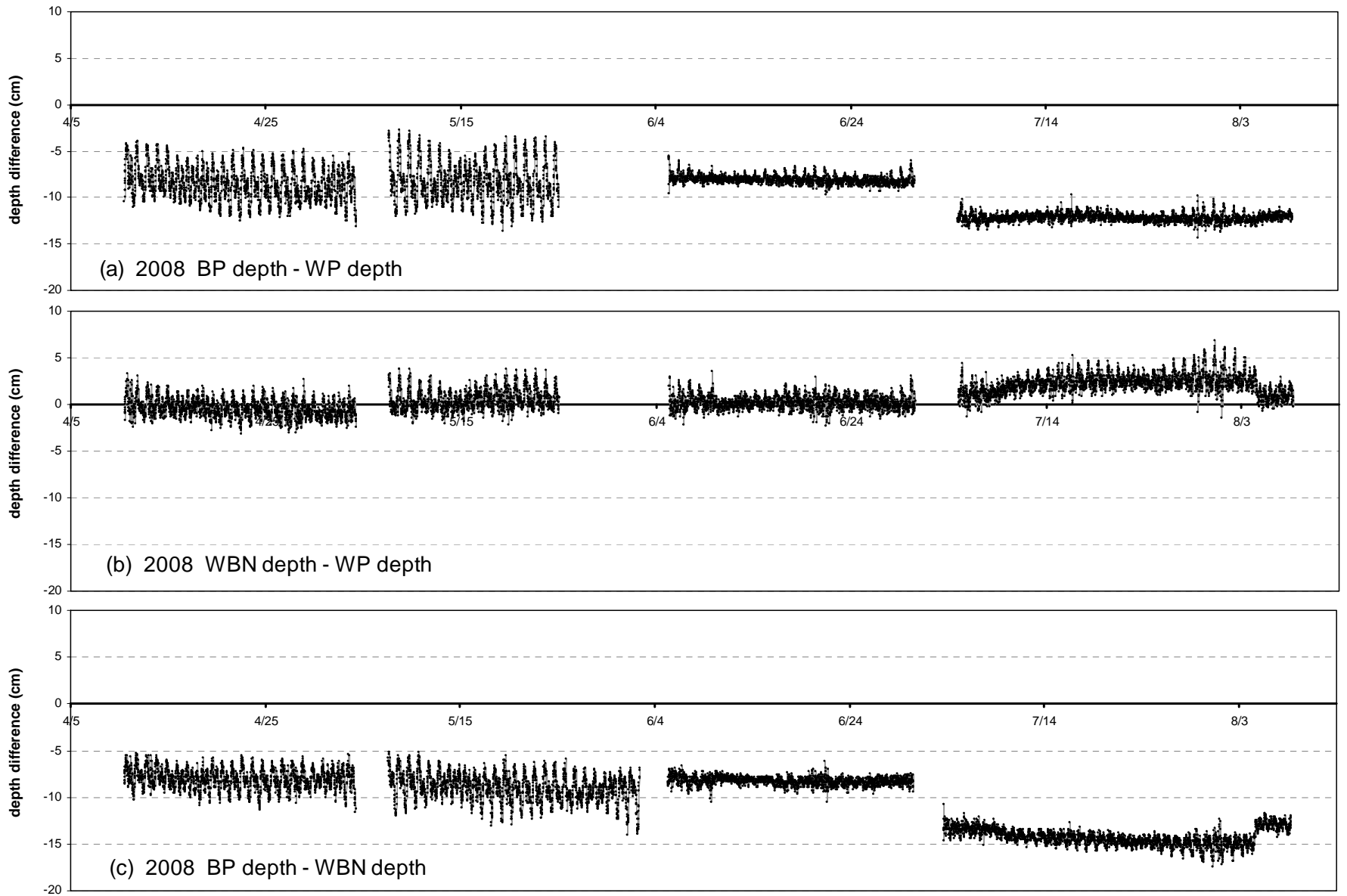


Figure A-4. 2008 time series of depth differences between paired stations.

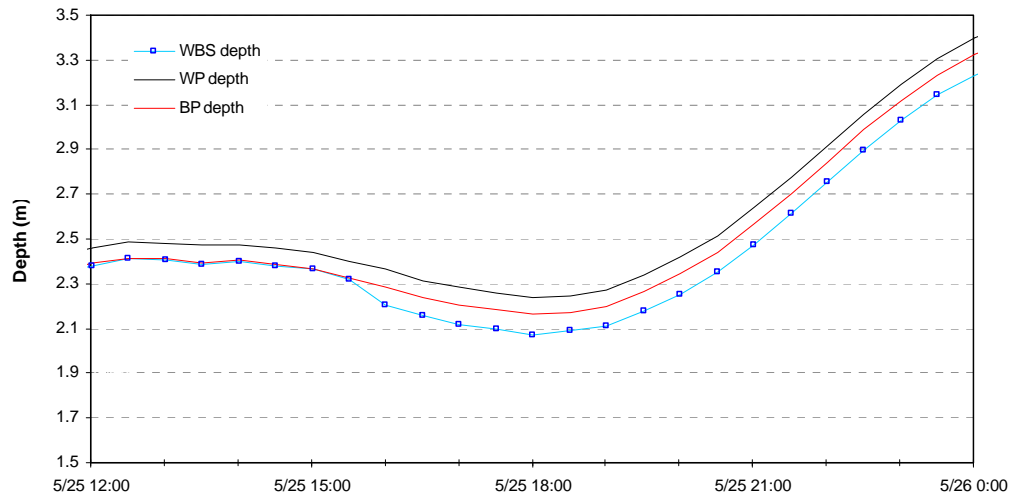


Figure A-5. Water depth over a 12-hour period on 25 May 2007. Between 15:30 and 16:00, the depth observed at WBS abruptly decreased by approximately 9 cm following retrieval and cleaning.

Many values in Figure A-2 cluster about -1.25 meters. We can adopt this as the target deployment depth that was intended. This is somewhat arbitrary but is useful in assessing the effects of departures from the target depth. Each deployment was assessed for significant departure from -1.25 meters depth using *t*-tests and the Holm-Bonferroni method to control for Type I error with repeated testing. Due to the large sample size for each test, most deployments had significant departures. While these were statistically significant, small departures may not be physically meaningful. A secondary criterion was applied in an attempt to isolate only physically meaningful departures – only departures greater than 3 cm were used to assess the effects of depth departures.

To assess the potential magnitude of the effect of these depth discrepancies on PAR observations, PAR values were adjusted for those deployments with significant (>3cm) departure from -1.25 m. Values were adjusted to approximate the values that would have been obtained at -1.25 m using the observed attenuation value, the magnitude of the depth departure and Beer’s Law. The cumulative adjusted PAR for 2007 and 2008 are shown in Figure A-6 and Figure A-7, respectively. These figures are directly comparable to Figure 3-10 (p.22) and Figure 3-11 (p.23), respectively. The most notable effect of the depth adjustment is that WP cumulative PAR is adjusted upwards relative to the other stations. WP had the greatest cumulative PAR in 2008, compared to BP and WBN. In 2007, the WP value was very similar to the BP value as measured by the PAR2 sensors. BP still had higher cumulative PAR as measured by the PAR1 sensors in 2007.

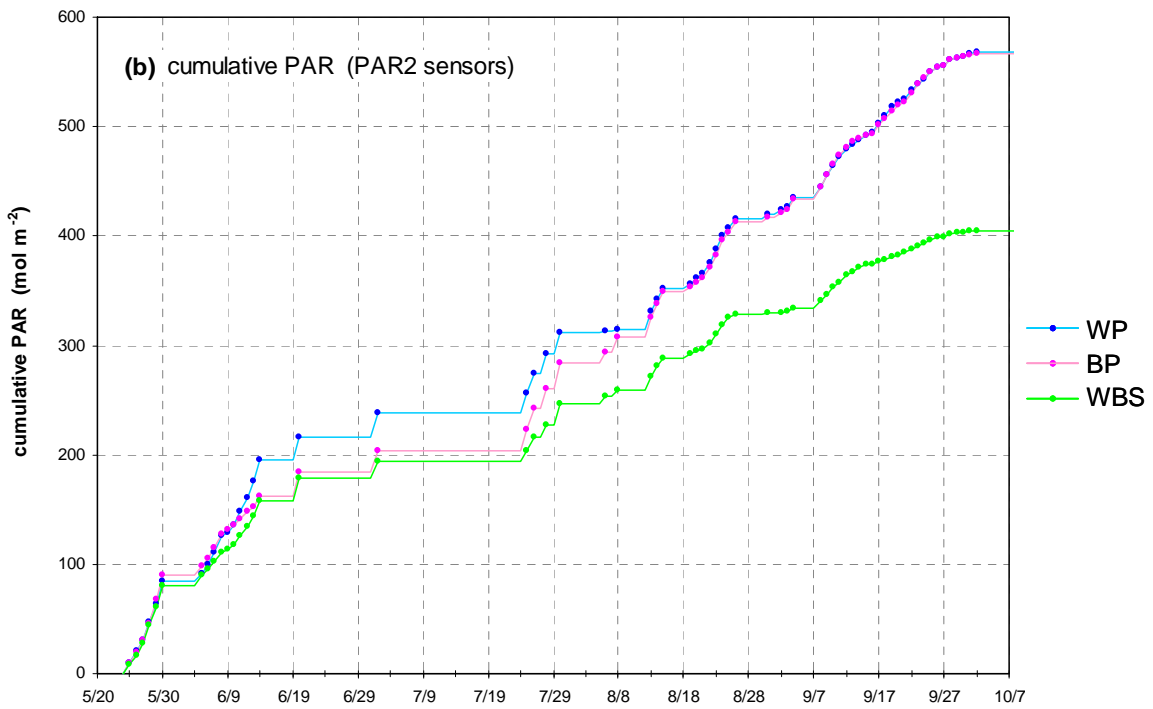
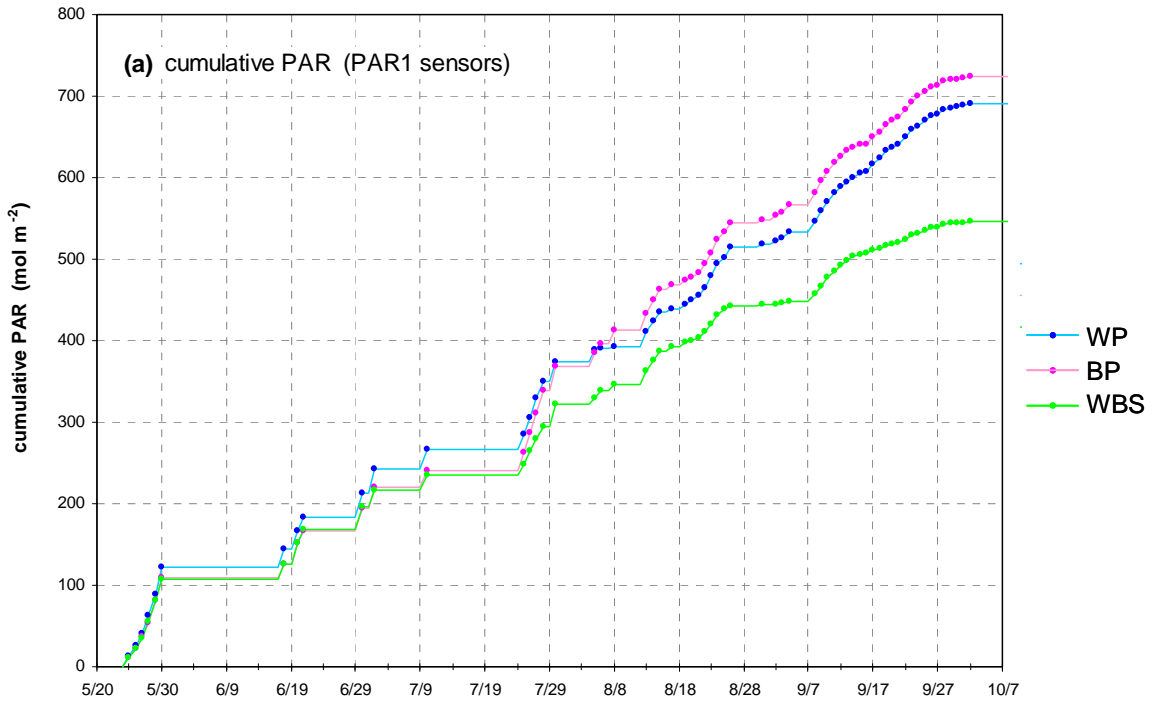


Figure A-6. 2007 cumulative PAR using depth-adjusted data. The depth adjustment elevated slightly the WP cumulative PAR values (compare to Figure 3-10, p.22).

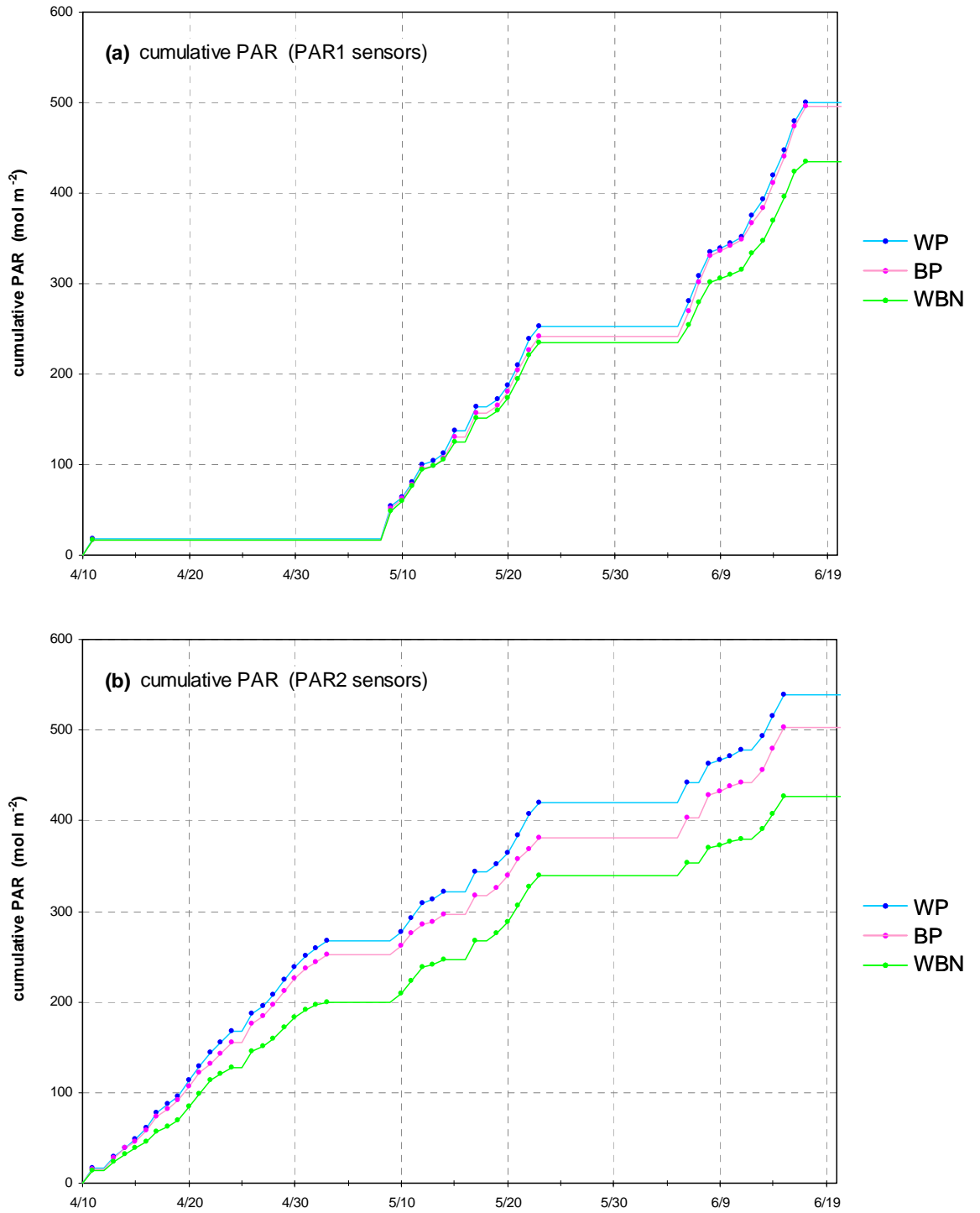


Figure A-7. 2008 cumulative PAR using depth-adjusted data. The depth adjustment elevated slightly the WP cumulative PAR values (compare to Figure 3-11, p.23).

The comparison of 2007-2008 average daily PAR at the three stations was repeated using the depth-adjusted data. Again, the main effect of the depth adjustment was to increase the values for WP (Figure A-8; compare to Figure 3-9, p.21). Repeated measures ANOVAs found significant differences between stations (Table A-1).

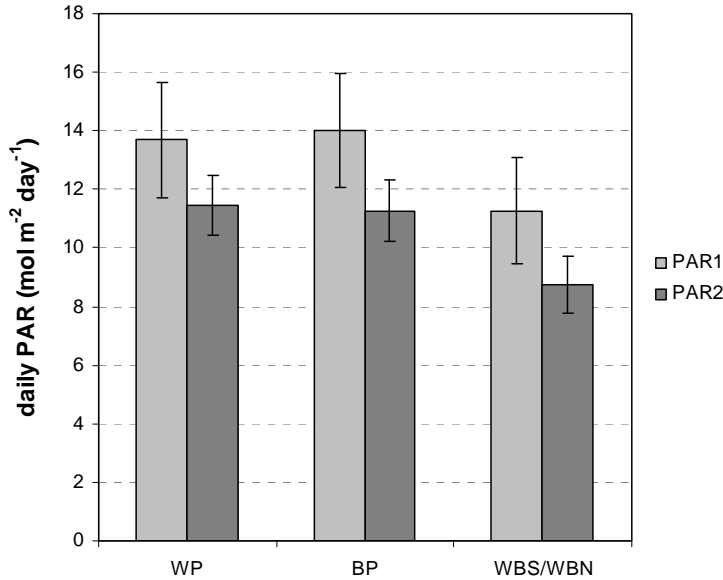


Figure A-8. Average 2007-2008 daily PAR for the Westcott Bay stations for each PAR sensor based on depth-adjusted data. Only days with contemporaneous data across the stations were included in the averages. The stations at the head of the bay (WBS and WBN) were treated as a single station. Error bars are 95% confidence intervals.

PAR1 ANOVA

Source of Variation	SS	df	MS	F	P-value
Day	19831.04	86	230.5935	50.25641	0.000000
Station	393.6125	2	196.8062	42.89269	0.000000
Error	789.1945	172	4.58834		

PAR2 ANOVA

Source of Variation	SS	df	MS	F	P-value
Day	11797.66	128	92.169216	24.60825	0.000000
Station	594.7568	2	297.37839	79.39703	0.000000
Error	958.8377	256	3.7454597		

Table A-1. Repeated measures ANOVA tables testing for significant differences ($\alpha=0.05$) between stations in daily PAR based on depth-adjusted data. All days (2007 and 2008) with contemporaneous data across the three stations were included in the analyses. These ANOVAs were run as two-way ANOVAs without replication with the day as the factor without replication.

The ANOVAs were followed up with Tukey tests to determine which specific station differences were significant (Zar 1999, p.210). The depth adjustment resulted in WP and BP stations being indistinguishable in terms of average daily PAR (Table A-2). Earlier, the tests conducted on unadjusted data found equivocal results – BP was found to have higher average daily PAR as measured by the PAR1 sensors, but the stations were indistinguishable base on PAR2 data (Table 3-5, p.20).

Station comparison	PAR1 results	PAR2 results
WP vs WBS/WBN	Reject H_0	Reject H_0
BP vs. WBS/WBN	Reject H_0	Reject H_0
WP vs BP	Accept H_0	Accept H_0

Table A-2. Results of Tukey mulicomparison tests in follow-up to the significant ANOVA results (Table A-1). In each case, the null hypothesis tested, H_0 , states that average daily PAR was equivalent at the two stations tested. All tests performed with $\alpha=0.05$. Compare these results to Table 3-5 (p.20) where the WP vs. BP comparison found a significant difference (BP higher) based on unadjusted PAR1 data.

A.2 Unattached Sensor

When the WP instrument was retrieved in June 2007 for routine servicing, the upper PAR (PAR1) sensor was found unattached from its bracket and downward facing. The strongly reduced PAR observations are obvious in the data for the preceding deployment and this data was removed (deployment 2a in Figure 3-1, p.12).

A.3 Reversed PAR Connections

The second major problem with the PAR data became apparent when inspecting attenuation results calculated from the upper and lower PAR sensors. It appeared that for some data segments, the attenuation values were predominantly negative. This suggested that the cables for the upper (PAR1) and lower (PAR2) sensors had possibly been reversed. By the time this was noticed, the instruments had been disassembled and could not be inspected. To investigate this possibility of cable reversal, the average attenuation coefficient and the fraction of negative values were calculated by deployment period (Figure A-9).

There were four deployments at WP (4, 6, 7 and 8) that produced data consistent with switched PAR cables. The magnitude of the averages for these four deployments is comparable to the magnitude of the first two WP deployments but of opposite sign. In addition, the same instrument was used for each of these deployments, which would be expected if the sensors were wired incorrectly when the instrument was first assembled.

Two other deployments have negative average attenuation: deployment 5 at WP (-0.01 m^{-1}) and deployment 4 at BP (-0.2 m^{-1}). It seems unlikely that these deployments had switched cables for the following reasons. The variability in attenuation for these two deployments is large (as measured by the standard error) suggesting that other instrument problems may have introduced noise into the data. Deployment 4 at BP used the same instrument that produced positive average attenuation in other deployments at BP, and it was unlikely that the instrument was rewired in the field. Furthermore, while these two deployments have a substantial fraction of negative attenuation estimates (Figure A-9), these fractions are markedly lower than those for the WP deployments where cables are believed to have been switched.

The frequency histograms of attenuation provide further support for concluding that only deployments 4, 6, 7 and 8 at WP had switched cables. These are the only four deployments that produced a distribution of attenuation coefficients with a negative mode (Figure A-10). The other two deployments with negative mean attenuation had positive modes, but large numbers of very negative attenuation values that likely indicates some other instrument problem that produced bad data. This is particularly noticeable in deployment 4 at BP.

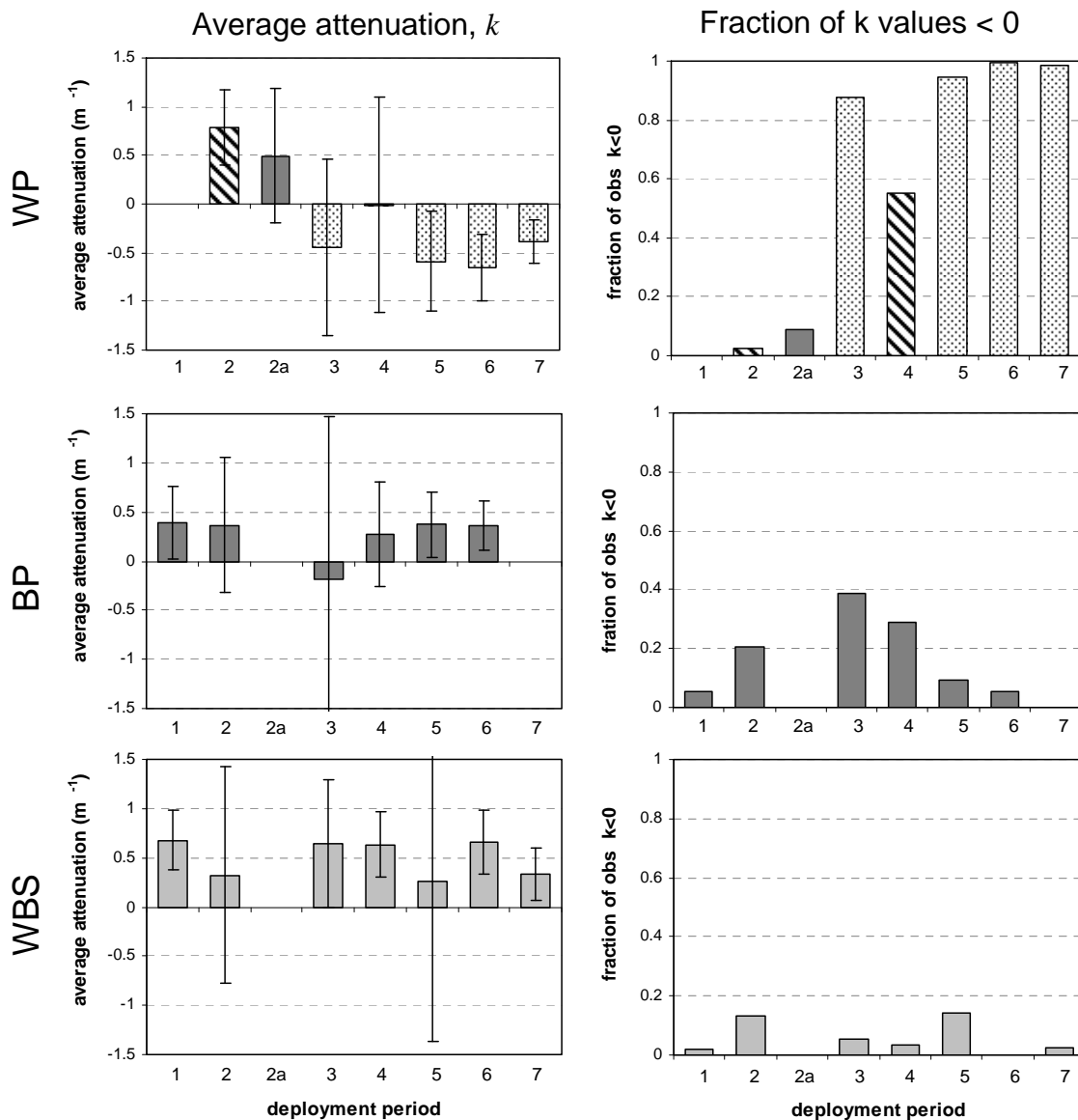


Figure A-9. Average calculated light attenuation (\pm s.e.) and the fraction of attenuation values that were less than zero, by deployment period. The shading or fill pattern for each bar indicates a specific YSI instrument (see Figure 3-1, p.12).

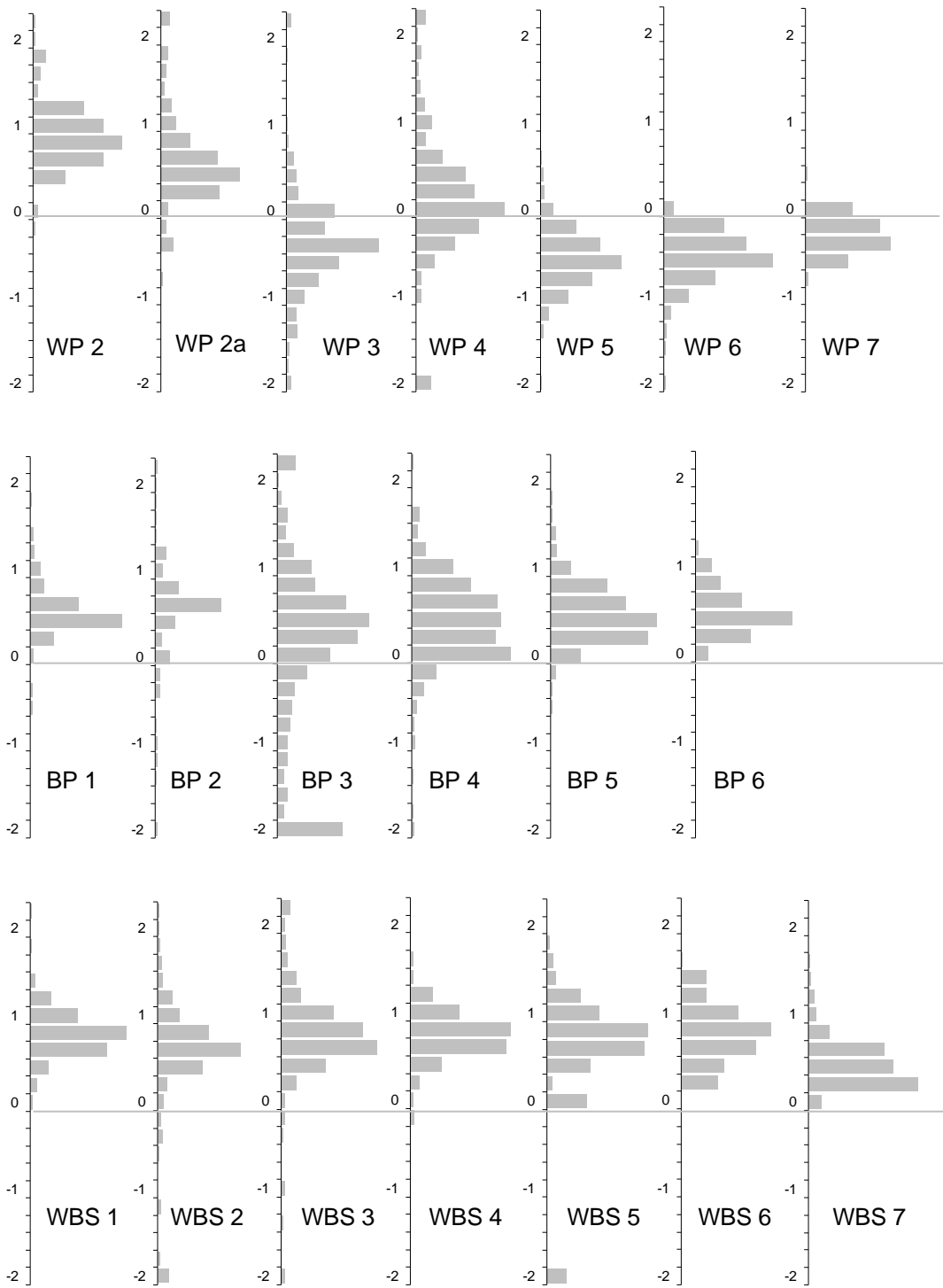


Figure A-10. Frequency histograms of calculated attenuation coefficient for the WP (top), BP (middle) and WBS deployments (bottom). The y-axis is attenuation coefficient in m^{-1} .

A.4 PAR Sensor Error Analysis

Before concluding that the PAR cables were switched for the WP deployments 4, 6, 7 and 8 (section A.3), we must consider the possibility that instrument errors caused the negative attenuation values. In addition to the absolute calibration error typically seen in Li-Cor LI-192 instrument specifications, several other error terms are discussed by Biggs (2000). Only the larger error terms are considered here (Table A-3).

Error Term	Magnitude
Absolute calibration error	±5%
Spectral response error	±5%
Immersion error	±2%
Cosine error	±2%

Table A-3. Estimated error terms associated with the Li-Cor LI-192 (Biggs 2000).

The calibration error is associated with the lamp used for calibration and other calibration conditions (e.g. stray light). The immersion error is due to the fact that Li-Cor calibrates in air and applies a typical immersion correction factor which may vary between sensors. The cosine error is the departure of the sensor response from Lambert's cosine law. Li-Cor gives estimates of other error terms (Biggs 2000), but these are much smaller in magnitude and are neglected here.

Error associated with sensor drift can also be important but is ignored here since these instruments were deployed within a few months of Li-Cor calibration in March 2007. It is reasonable to assume that the error terms are independent. A total error is then estimated as the square root of the sum of squared error terms: total error = ±7.6%. Figure A-11 translates this into an absolute error term in $\mu\text{mol m}^{-2} \text{s}^{-1}$ for a range of irradiance levels.

The error associated with PAR measurements will propagate to calculated attenuation. This propagation of error can be estimated using the approach of Bevington (1969). First, we manipulate the equation for calculating attenuation (k) from irradiance measured by the PAR1 (I_{PAR1}) and PAR2 (I_{PAR2}) sensors:

$$I_{PAR2} = I_{PAR1} e^{-kd}$$

$$k = -\frac{\ln\left(\frac{I_{PAR2}}{I_{PAR1}}\right)}{d}$$

$$k = \left(-\frac{1}{d}\right)\ln(I_{PAR2}) + \left(\frac{1}{d}\right)\ln(I_{PAR1}) \quad (\text{Eq.A1})$$

where d is the distance of the vertical separation between the two sensors. The value of d is 40.5 cm for all instruments in 2007 except for 07C1026 AB which has a value of 39.0 cm.

If we assume that the errors in the PAR1 and PAR2 sensors are independent (uncorrelated), then we can invoke the general equations for propagation of error for a sum and logarithm (Bevington 1969, pp.60-64).

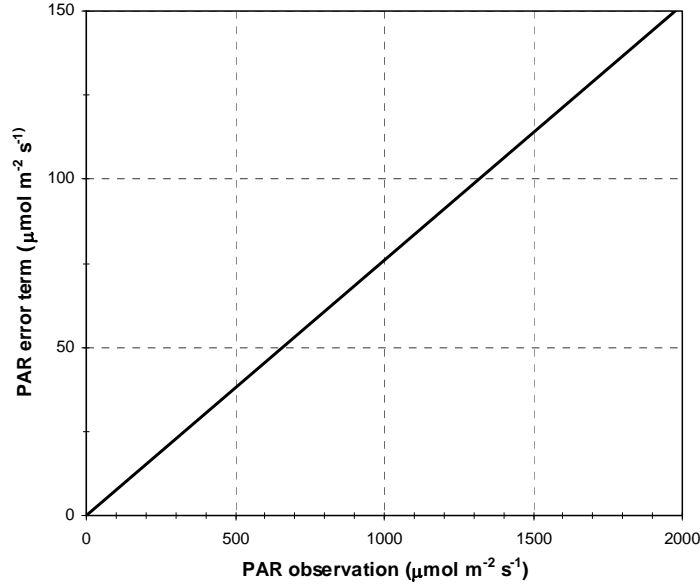


Figure A-11 Systematic error as a function of the magnitude of PAR observation for an estimated total systematic error of $\pm 7.6\%$.

If x is the sum of u and v weighted by constants a and b ,

$$x = au + bv,$$

then the errors associated with u and v (σ_u and σ_v , respectively) propagate to x as (Bevington 1969, Eqn. 4-10)

$$\sigma_x^2 = a^2 \sigma_u^2 + b^2 \sigma_v^2. \quad (\text{Eq.A2})$$

Similarly, if u is the logarithm of w multiplied by constant c ,

$$u = c \ln(w),$$

then the error associated with w (σ_w) propagates to u as (Bevington 1969, p.64)

$$\sigma_u = c \frac{\sigma_w}{w}. \quad (\text{Eq.A3})$$

Combining equations (A1), (A2) and (A3), the total error on PAR observations propagates to k estimates as

$$\sigma_k^2 = 2 \frac{r^2}{d^2}, \quad (\text{Eq.A4})$$

where σ_k is the error associated with k estimates and r is the total error associated with PAR observations on a relative basis (i.e. $\sigma_l = rI$, where I is PAR irradiance and σ_l is the absolute error associated with I). Using the value of $r=0.076$ (7.6%) produced above,

$$\sigma_k = 0.27 \text{ m}^{-1}.$$

This error on k estimates is analogous to the total error on PAR observations, in that it represents an upper limit on the magnitude of the error that can be expected using a specific sensor. For example, Li-Cor presents the $\pm 5\%$ calibration error as a conservative (large) estimate with typical errors at $\pm 3\%$ (Biggs 2000, p.3). In a qualitative sense, it therefore seems reasonable to think of these errors as two times or even three times value of the standard deviation (of the frequency distribution of errors found with a sample of different sensors), rather than, for example, the standard deviation itself. In the context of a normal distribution, an interval constructed using the error estimate would then encompass 95% or 99% of the total distribution (if the error is $2\times$ or $3\times$ the standard deviation, respectively).

The only purpose for being this explicit about the nature of the error is to help evaluate the likelihood that the negative modes in the attenuation distributions (Figure A-10) are attributable to instrument (systematic) error. This analysis suggests that lower limit of negative attenuation estimates that could be attributed to instrument error is approximately $k = -0.27 \text{ m}^{-1}$. This scenario assumes that true attenuation is near zero and actual instrument error is at its extreme lower limit, which, depending on the frequency distribution of errors, may not be very likely. The greatest numbers of attenuation estimates for WP deployments 6 and 7 were in the $-0.4 \text{ m}^{-1} < k < -0.6 \text{ m}^{-1}$ bin (Figure A-10). These values are more negative than the extreme scenario with instrument error, making it highly unlikely that these values are negative as a result of instrument error. It therefore seems most likely that the PAR sensor cables were switched on instrument 07C1026 AC that was used in 2007 for WP deployments 4, 6, 7 and 8 (Figure 3-1, p.12).

A.5 Correction for Reversed PAR Connections

Proceeding under the assumption that the PAR cables on instrument 07C1026 AC were switched, then the input signals from the upper and lower sensors were reversed and the incorrect calibration coefficients were applied to these signals.

The raw signal from the LI-192 is converted within the YSI sonde to quantum flux units simply by multiplication with a calibration multiplier. The multiplier specified on Li-Cor calibration sheets in units of $\mu\text{mol m}^{-2} \text{ s}^{-1} \mu\text{A}^{-1}$ must be multiplied by $-1/100$, as per YSI instructions², to produce the value to be entered into the YSI instrument.

² These instructions are given in the 6-page YSI manual that arrived with the instruments and is titled "Wiped PAR Addendum".

Sensor Position on Instrument 07C1026 AC	Li-Cor LI-192 Serial Number	Li-Cor Calibration Multiplier (Li-Cor calibration on 3/5/07)	YSI Sonde Parameter For Internal LI-192 Signal Conversion
PAR1 (upper)	UWQ 7271	-295.97 $\mu\text{mol m}^{-2} \text{s}^{-1} \mu\text{A}^{-1}$	2.9597
PAR2 (lower)	UWQ 7270	-317.30 $\mu\text{mol m}^{-2} \text{s}^{-1} \mu\text{A}^{-1}$	3.1730

Table A-4. PAR sensor calibration multipliers for LI-192 sensors on YSI instrument 07C1026 AC.

The uncorrected data (denoted with superscript v1) was corrected in the version of the data denoted v2 as follows:

$$I_{PAR1}^{v2} = \left(\frac{I_{PAR2}^{v1}}{3.1730} \right) (2.9597)$$

$$I_{PAR2}^{v2} = \left(\frac{I_{PAR1}^{v1}}{2.9597} \right) (3.1730)$$

A.6 Out-of-Water Observations

When the YSI instruments were deployed it was recognized that at very low tides, the upper PAR sensor might be exposed to air. This was observed and documented in the field on 6/15/07 (Figure A-12).

Emersion of the upper sensor fundamentally changes the nature of the PAR data (Kirk 1994). The effects of reflection and scattering at the air-water interface are eliminated from the PAR1 observation and introduced as a confounding difference between the PAR1 and PAR2 observations (assuming the PAR2 sensor remains submerged). During initial inspection of the PAR1 data, some spikes were apparent that might be consistent with emersion. For these reasons, the frequency of emersion was assessed on the basis of the observed 6/15/07 emersion event and Westcott Bay tide level estimates for the entire study period.

Field notes recorded by Anja Schanz reflect the extent of the 6/15/07 emersion event that was observed at the WP station (shown in Figure A-12):

9:40 – 9:50 PDT	PAR1 sensor under water
10:20 PDT	PAR1 sensor exposed to air
10:50 PDT	PAR1 sensor exposed to air
11:10 PDT	PAR1 sensor began to be covered by water



Figure A-12. Photo of upper PAR sensor at WP in air during a low tide at 10:25 PDT 6/15/07.

Either YSI depth observations or a tide time series could be used to identify potential emersion events across the study period. There is error associated with each of these. Errors on depth observations arise from variations in deployment depth across the stations as well as the effects of variable atmospheric pressure over the study period. Observed atmospheric pressure at Friday Harbor varied by 34 mb (3400 Pa) over the 2007 study period, which corresponds roughly with an apparent variation in depth observations of 34 cm (assuming average seawater density of 1025 kg m^{-3}). Estimates of tidal heights obviously suffer from distance to the nearest tidal observations (Friday Harbor). Nevertheless, estimates of tidal heights were used as the basis for identifying potential emersion events.

The tides in Westcott Bay were estimated as follows for the 2007 and 2008 sampling periods. The mean 15-minute predicted tides (Nobeltec Tides & Currents) for Roche Harbor and Hanbury Point were averaged to produce a predicted tide for Westcott Bay. This predicted tide was adjusted by the departure of the observed tide at Friday Harbor (<http://tidesandcurrents.noaa.gov>; station 9449880; hourly observations interpolated to 15 minute values) from the predicted tide at Friday Harbor (also predicted by Nobeltec Tides & Currents).

The estimated tides correspond fairly well to the field observations of water column depth (Figure A-13) but there is clearly some temporal displacement. Nevertheless, this comparison suggests that with tides of approximately -0.9 m MLLW or higher, emersion of the PAR1 sensor should not be a concern for this particular deployment at WP.

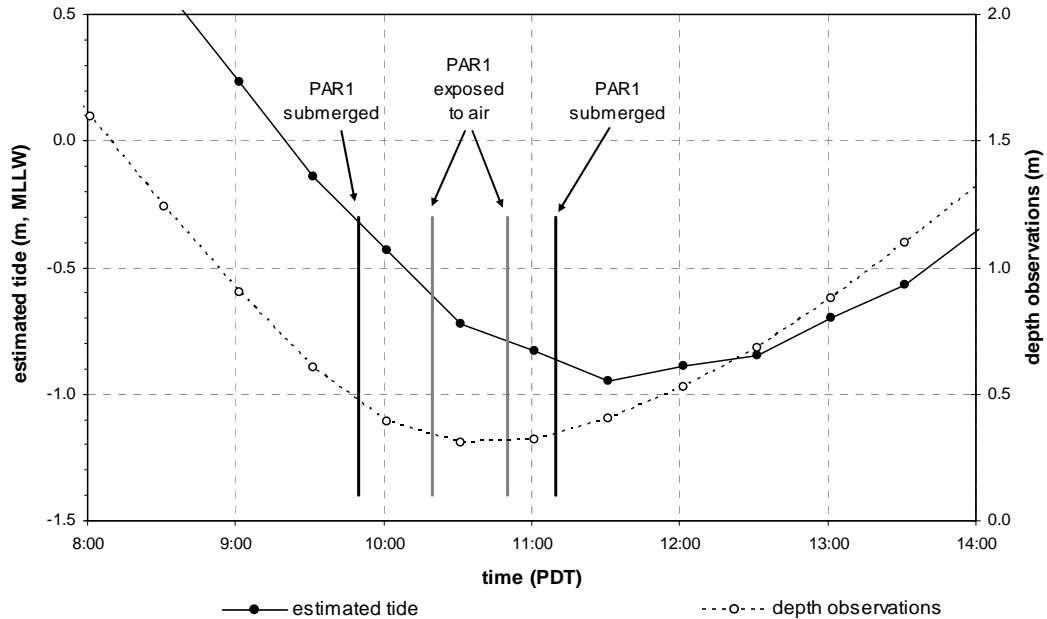


Figure A-13. Westcott Bay tides on 6/15/07 estimated at 30 minute intervals and the time of discrete field observations of PAR1 sensor submersion and emersion at the WP station (vertical lines). The YSI depth observations at WP are also shown.

The estimated differences in deployment depths (Figure A-2, p.46) can be used to translate this emersion threshold to the other deployments and the other stations. The resultant emersion thresholds are overlaid on the estimated tides in Figure A-14.

In the 2007 data, emersion effects are only a concern in the mid-June low-tide series. During the May low-tide series, the instruments had been retrieved for servicing and were not deployed. The low tides in October were all night time low tides, and therefore not a concern for PAR measurements. A closer look at the June tide series shows there are a few data points in the WP and WBS PAR1 data that are potential emersion artifacts – i.e., spikes or elevated values in PAR1 that are not accompanied by a similar pattern in PAR2 (Figure A-15). Some potential emersion artifacts were removed in the automated cleanup process (Appendix B).

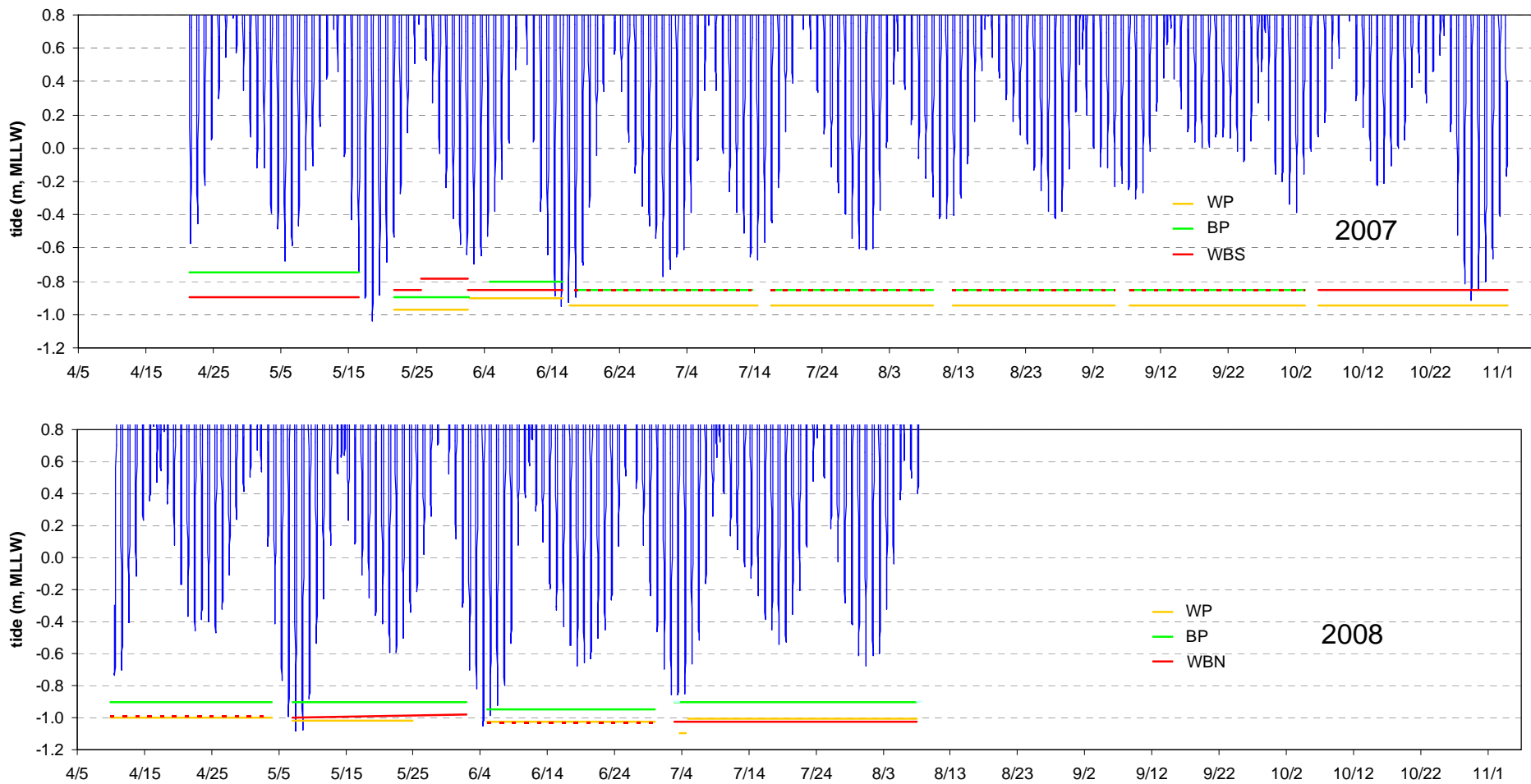


Figure A-14. Estimated tides at Westcott Bay throughout the 2007 and 2008 sampling periods and the approximate thresholds for PAR1 emersion for each deployment and each station.

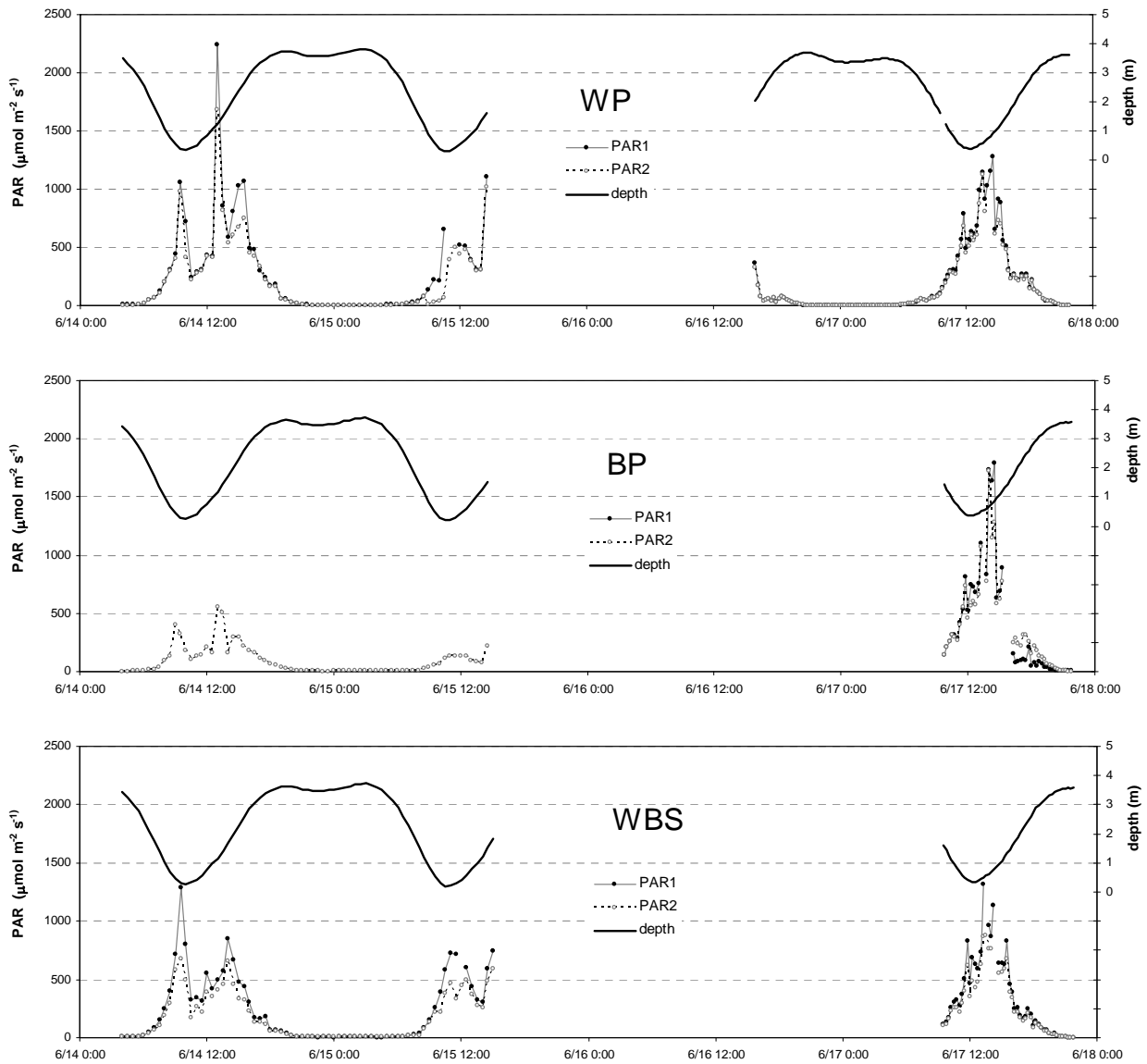


Figure A-15. Cleaned PAR and water depth measurements during the June 2007 low tide series. PAR1 sensor emersion was observed at WP at 10:30 on 6/15/07 and most likely occurred at other times during this tide series.

Data from the May 2008 tide series includes elevated PAR1 observations at all three stations that are likely associated with emersion (Figure A-16).

Overall, the extent of emersion in the data is very restricted, and where it does occur the data are not elevated in all cases. The effects of emersion on the PAR analyses appear to be negligible and are not considered further.

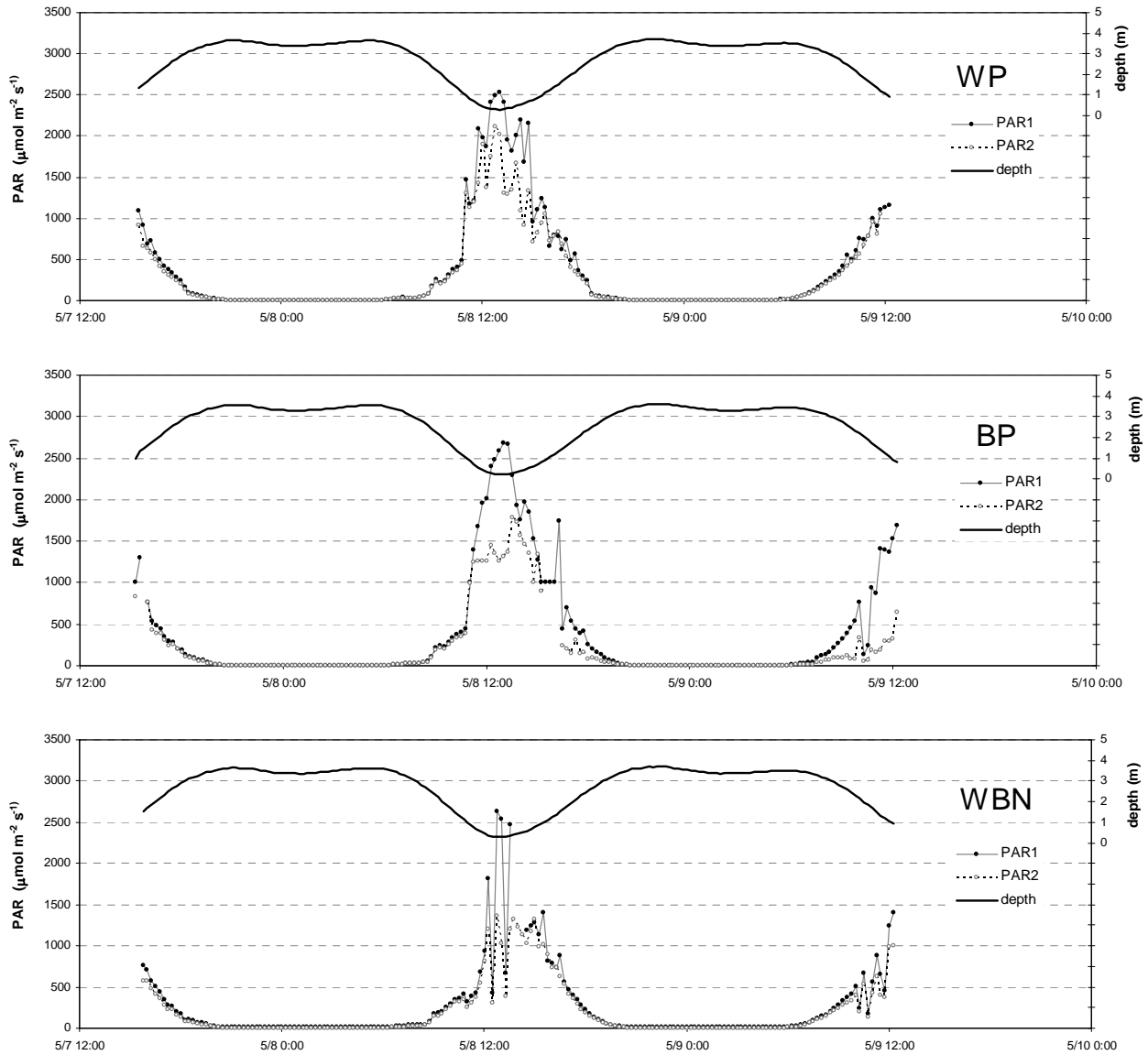


Figure A-16. Cleaned PAR and water depth measurements during the May 2008 low tide series that likely included emersion of the PAR1 sensors.

A.7 References

Bevington, P.R., 1969, **Data Reduction and Error Analysis for the Physical Sciences**, McGraw-Hill, 336pp.

Biggs, W.W., 2000, **Principles of Radiation Measurement**, a Li-Cor technical report excerpted from Gensler, W.G. (ed.), 1984, *Advanced Agricultural Instrumentation*, Proceedings from the NATO Advanced Study Institute on *Advanced Agricultural Instrumentation*. Accessed online (4/9/08):
http://www.licor.com/env/Products/Sensors/lightensors_brochures.jsp

Zar, J.H., 1999, **Biostatistical Analysis**, 4th edition, Prentice-Hall.

Appendix B PAR Data Cleanup

B.1 PAR Data Anomalies

After the issues discussed in Appendix A were addressed, the PAR data and calculated attenuation were inspected at a fine resolution (variation with time-of-day). Three patterns were apparent that were considered anomalies – i.e. non-physical artifacts or unintended measurement conditions.

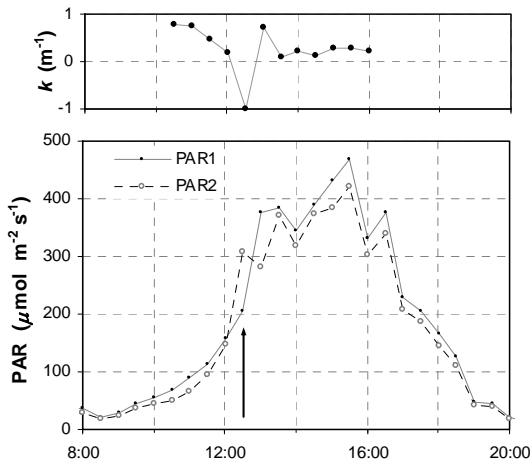
- (1) There was a high occurrence of negative attenuation with values too low to be explained by systematic error in the Li-Cor sensor (i.e. $k < -0.27 \text{ m}^{-1}$, section A.4, p.57). See Figure B-1(a) through (d).
- (2) While the PAR1 and PAR2 observations were generally expected to have incremental change of the same sign, there were many observations with changes of different sign. See Figure B-1(b).
- (3) There were a small number of days where the mid-day PAR values abruptly fell to near-zero values and showed little or no variation for several measurements before abruptly returning to values of the expected magnitude and following an expected pattern of change. See Figure B-1(d).

Figure B-1(b) illustrates that in some cases there is overlap in categories (1) and (2) – i.e. incremental change of opposite sign in PAR1 and PAR2 is coupled with a non-physical negative attenuation result. However, this is not always the case.

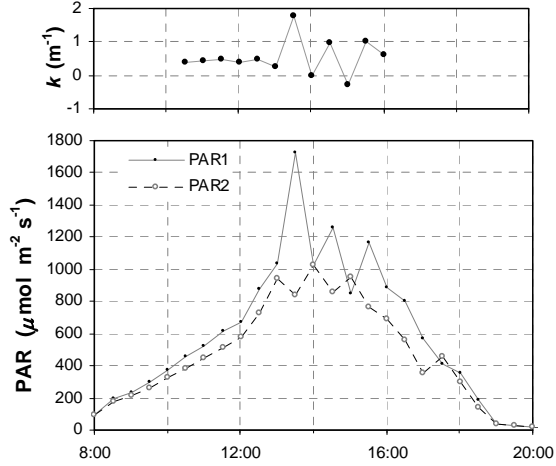
The causes of these anomalies are unknown, but likely involve instrument random errors or sensor obstruction. The instrument random errors could either be associated with the finite precision of the Li-Cor sensor, or the electronics of the YSI data capture system. Sensor obstruction could be caused by water column debris or intermittent covering of the sensor by biofouling growth on the deployment apparatus or by detached plant material that temporarily rests on the instrument.

The variability in PAR measurements in dark conditions (within a window around solar mid-night) was used for a limited assessment of instrument random error. The premise was that in conditions where available PAR was negligible, environmental variability will also be negligible and any existing variability can be attributed to the instrument. The actual patterns in nighttime PAR cannot be completely explained (Figure B-2). In some data segments, PAR1 and PAR2 are both unvarying but with different levels of displacement from $0 \mu\text{mol m}^{-2} \text{ s}^{-1}$. These departures from zero likely reveal differing systematic errors (including calibration error) between the two sensors. These segments suggest that the accuracy reported by Li-Cor as a proportion of the reading does not truly reflect accuracy in very low readings – i.e. the error does not approach zero as the readings approach zero. The variability in other data segments does not seem periodic, but

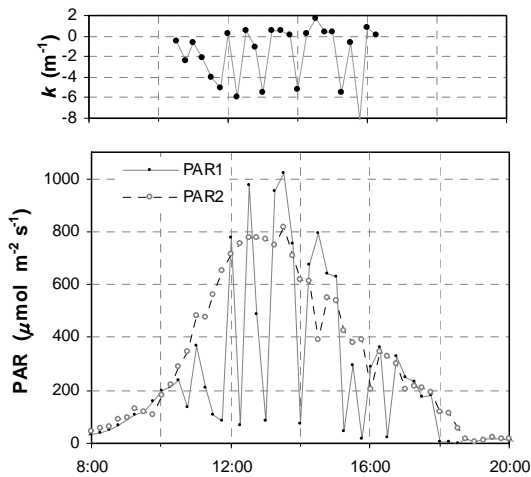
(a) June 5: non-physical negative attenuation ($k < -0.27 \text{ m}^{-1}$) at 12:30.



(b) May 22: incremental change of opposite sign in PAR1 and PAR2. Data from 15:00 also reflects non-physical attenuation.



(c) August 1: extensive instability in PAR1 resulting in non-physical attenuation.



(d) July 5: abrupt mid-day loss of signal in both PAR1 and PAR2.

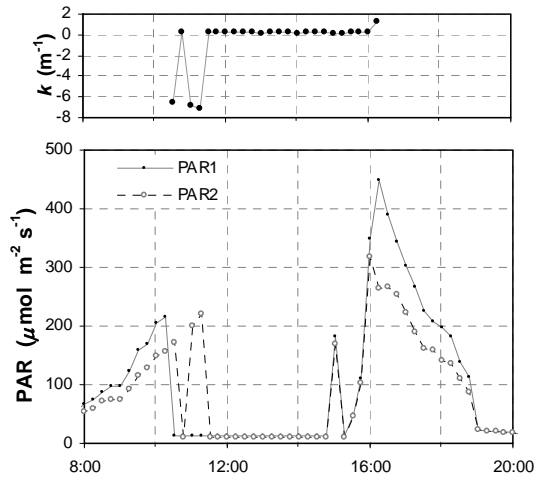


Figure B-1. Examples of different modes of data anomalies taken from the WP data record from 2007. For each example, the plot of PAR1 and PAR2 is paired with a plot of the resultant attenuation. Note that the scales vary on the y-axes.

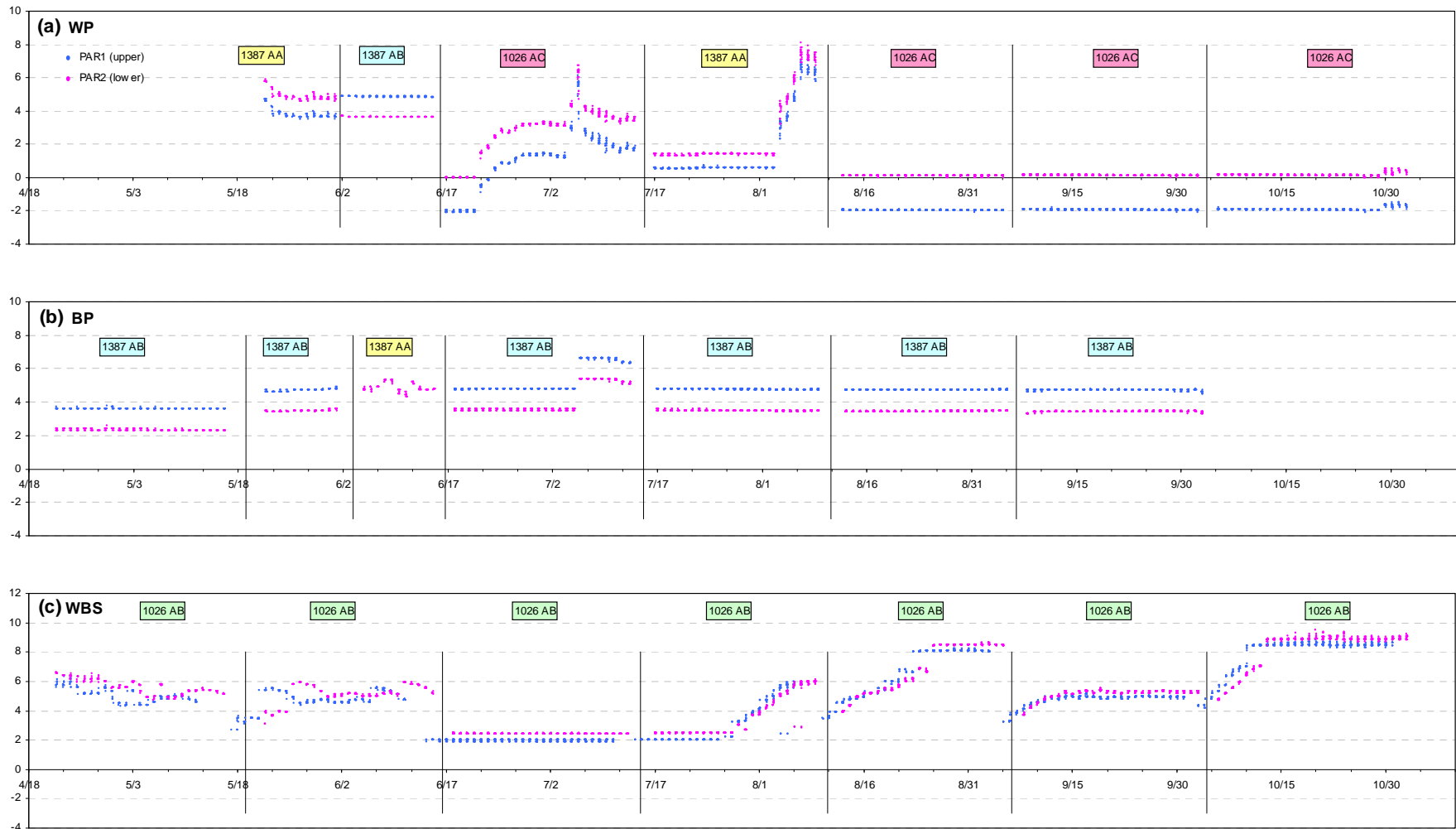


Figure B-2. 2007 nighttime PAR data (in $\mu\text{mol m}^{-2} \text{s}^{-1}$) for WP, BP and WBS. Only data within a 6-hour window centered on solar midnight is shown. Vertical black lines indicate instrument maintenance and delineate discrete deployments. The colored boxes along the top indicate which instrument was used for each deployment.

does show non-random pattern over the course of many days. This variability possibly represents noise from the electronics of the data processing and logging system.

If electrical noise is introduced into the signal, then it is possible that some PAR measurements would be greater than could realistically be expected. If such high values are present this could be taken as further evidence of noise introduced from the YSI electronics. The maximum PAR values measured during this study are shown in Table B-1.

	WP	BP	WBS
PAR1 sensors	2,639	2,315	2,732
PAR2 sensors	1,685	1,723	1,536

Table B-1. Maximum PAR values measured over the 2007 study period, in $\mu\text{mol m}^{-2} \text{s}^{-1}$.

To quantify the maximum feasible PAR measurements, an in-air PAR data record collected at UW Friday Harbor Labs (FHL) was acquired (courtesy Emily Carrington’s lab, http://depts.washington.edu/fhl/fhl_wx.html). This data was collected with a Campbell Scientific weather station. The maximum value of PAR measured over the entire dataset available at the time of analysis, which encompasses the study period, (7/28/06 – 4/30/08) was $2,192 \mu\text{mol m}^{-2} \text{s}^{-1}$. The maximum value measured in Westcott Bay, $2,732 \mu\text{mol m}^{-2} \text{s}^{-1}$, is 25% above the maximum in-air value measured at FHL. This suggests the presence of spurious positive departures, but this is not a definitive comparison because the uncertainty in the FHL data has not been considered, and the WBS maximum data point was associated with minimal water column attenuation (low tide on 6/30/07 10:46; see Figure A-14, p.63). Still, the occurrence of positive departures relative to the FHL in-air data suggests there may be noise in the YSI hardware.

A rough, theoretical calculation of the absolute maximum expected surface (out-of-water) PAR measurements can provide another check on the plausibility of the values in Table B-1. The total solar radiation incident at the top-of-atmosphere (known as the solar constant) is approximately $\Phi=1367 \text{ W m}^{-2}$ (Iqbal 1983, p.49). The greatest total solar radiation at the earth’s surface will occur with the sun directly overhead. In this case the direct solar radiation at the earth’s surface is estimated as the product $\Phi \cdot \tau$, where τ is the atmospheric transmissivity to solar radiation. For “clear sky” conditions, τ can reach upper values of $\tau=0.7$, which results in surface direct radiation of $I_s = 957 \text{ W m}^{-2}$ (Jones 1992, p.24). Under these conditions, diffuse radiation is on average approximately 20% of global radiation (Jones 1992, p.25), so that the peak global solar radiation (direct+diffuse) at the earth’s surface is estimated as $1,196 \text{ W m}^{-2}$. PAR constitutes about 45% of solar direct beam radiation (Kirk 1994, p.30; Monteith and Unsworth 1990, p.38), but when diffuse sky radiation is considered this proportion is closer to 50% (Jones 1992, p.21). Peak PAR at the earth’s surface is then approximately 598 W m^{-2} .

This value in radiometric units (W m^{-2}) is converted to quantum units by first calculating the mean frequency of a PAR photon,

$$\nu = c/\lambda = (3.0 \times 10^8 \text{ m s}^{-1}) / (0.55 \times 10^{-6} \text{ m}) = 5.45 \times 10^{14} \text{ s}^{-1},$$

where c is the speed of light and λ is the wavelength of photon in the mid-PAR band. The approximate energy can then be calculated from Planck's Law for a single PAR photon,

$$E = h\nu = (6.63 \times 10^{-34} \text{ J s})(5.45 \times 10^{14} \text{ s}^{-1}) = 3.62 \times 10^{-19} \text{ J}$$

and for a mole of photons,

$$E_m = (E)(N_A) = (3.62 \times 10^{-19} \text{ J})(6.022 \times 10^{23} \text{ mol}^{-1}) = 217,777 \text{ J mol}^{-1}$$

Peak PAR at the earth's surface in quantum units is then approximately

$$(598 \text{ W m}^{-2})(217,777 \text{ J mol}^{-1}) = 2,746 \mu\text{mol m}^{-2} \text{ s}^{-1}.$$

This value is only slightly higher than the value recorded at WBS $2,732 \mu\text{mol m}^{-2} \text{ s}^{-1}$. While it seems unlikely that the WBS measurement is essentially equal to the absolute maximum possible value, we cannot dismiss it a non-physical value.

Ultimately, identifying the causes of the anomalies in the data records is beyond the scope of this report. The objective here is to characterize the anomalies to the extent necessary so that they can be isolated and treated separately in the data analysis and interpretation.

B.2 Cleanup Algorithm

This section describes the approach for identifying questionable PAR data points. These data points were replaced with "bad data" flags (-9999) in the cleaned dataset.

For each sampling time i on day j , we can define the following variables:

$I_{1,i}$, $I_{2,i}$ = measured PAR at PAR1 and PAR2 sensors at time i (subscript j dropped for simplicity)

k_i = attenuation calculated from PAR1 and PAR2 measurements (section 2.5, p.10),

$I_{1,j}^{\max}$, $I_{2,j}^{\max}$ = maximum daily PAR measured on day j by PAR1 and PAR2 sensors,

$\left\{ \begin{array}{l} \Delta I_{1,i} = I_{1,i} - I_{1,i-1} \\ \Delta I_{2,i} = I_{2,i} - I_{2,i-1} \end{array} \right\}$ = increment in PAR1 and PAR2 from previous measurement at time $i-1$ to current measurement at time i ,

$F_{1,i}$, $F_{2,i}$ = data quality flags for the PAR1 and PAR2 measurements that can take values of 0 (flagged by algorithm as questionable data) or 1 (not flagged by algorithm).

Each PAR1 measurement, $I_{1,i}$, was evaluated and flagged as questionable data if one or more of the following three conditions was met:

1. Attenuation within a ± 3 hour window of solar noon was more negative than could be explained by systematic error (section A.4, p.57):

$$k < -0.27 \text{ m}^{-1}$$

Solar noon was calculated on a daily basis as the midpoint between Friday Harbor sunrise and sunset obtained in PST from the US Naval Observatory (http://aa.usno.navy.mil/data/docs/RS_OneYear.php).

2. For PAR values above low-light conditions ($I > 20 \mu\text{mol m}^{-2} \text{ s}^{-1}$), the PAR1 increment was strongly negative (magnitude greater than 10% of the daily PAR1 maximum), and the PAR2 increment was positive and based on good data (i.e. the previous PAR2 measurement was not flagged as questionable data):

$$\left[\begin{array}{l} \Delta I_{1,i} < (-1)(10\%) I_{1,j}^{\max} \\ \Delta I_{2,i} > 0 \\ F_{2,i-1} = 1 \\ I_{1,i} > 20 \mu\text{mol m}^2 \text{ s}^{-1} \\ I_{2,i} > 20 \mu\text{mol m}^2 \text{ s}^{-1} \end{array} \right]$$

3. For PAR values above low-light conditions ($I > 20 \mu\text{mol m}^{-2} \text{ s}^{-1}$), the PAR1 increment was negative, and the PAR2 increment was strongly positive (magnitude greater than 10% of the daily PAR2 maximum) and based on good data (i.e. the previous PAR2 measurement was not flagged as questionable data):

$$\left[\begin{array}{l} \Delta I_{2,i} > (10\%) I_{2,j}^{\max} \\ \Delta I_{1,i} < 0 \\ F_{2,i-1} = 1 \\ I_{1,i} > 20 \mu\text{mol m}^2 \text{ s}^{-1} \\ I_{2,i} > 20 \mu\text{mol m}^2 \text{ s}^{-1} \end{array} \right]$$

Each PAR2 measurement, $I_{2,i}$, was evaluated by an analogous set of conditions.

In addition to these algorithms, eight days were identified with mid-day signal loss (Figure B-1d) through manual inspection of the entire dataset.

B.3 References

Iqbal, M., 1983, **An Introduction to Solar Radiation**, Academic Press, Ontario, Canada, 390pp.

Jones, H., 1992, **Plants and Microclimate**, 2nd Edition, Cambridge University Press, Cambridge UK, 428pp.

Kirk, J.T.O., 1994, **Light & Photosynthesis in Aquatic Ecosystems**, Second Edition, Cambridge University Press, New York, 509pp.

Monteith, J.L. and M. Unsworth, 1990, **Principles of Environmental Physics**, Second Edition, Edward Arnold, London, 291pp.